Rasayely
Membrane Science International
https://rasayely-journals.com/index.php/msi
Vol 1(2); 24–43, 2022

Original Article Open Access

Intermediate Temperature Oxygen Selective Membrane Technology Based on δ-Bi_2O_3/Ag Cermet for Distributed Multigeneration in Eco-Settlements with Sustainable Development

V.V. Zyryanov[1,*]

[1]*Institute of Solid State Chemistry and Mechanochemistry, Siberian Branch, Russian Academy of Sciences, Novosibirsk, 630090 Kutateladze, Russian Federation*

[*]Author to whom any correspondence should be addressed; e-mail: vladinetta@gmail.com, Tel.: +79137404422. Fax: +73833322847

Received: 15 February 2022; Revised: 04 June 2022; Accepted: 20 June 2022; Published: 01 September 2022

Academic Editor: Mohd Hafiz Dzarfan Othman, Universiti Teknologi Malaysia, Malaysia

Abstract

Eco-settlements are active examples of sustainable development for mass dissemination with minimal consumption. However, in general, the goals of sustainable development are rarely achieved. The main reason for the failure of a promising project is the unreasonable focus on alternative energy sources. The sun and wind—as renewable energy sources—are not permanent. Yet, increasing their share of energy requires energy storage technology. A new approach to green carbon energy is proposed in the form of a technically feasible concept of Distributed Multigeneration (DMG), for which unclaimed carbon resources are practically unlimited. A waste-free, flexible process without environmental pollution can be developed using the best-known and novel technologies. This article discusses the advantages and issues associated with cermet membranes. The ideas of a smart oxygen membrane, understanding of degradation processes, optimization of the architecture and compositions of membrane materials, and a technically feasible roadmap for continuous membrane fabrication could drive success for a new version of ion transport technology. For the implementation of membranes in the energy sector, the required durability is 8,000 hours. Such durability can be achieved by periodic regeneration of the membranes after the ordering of oxygen vacancies with short-term heating up to 640°C. Environmentally essential, full cleaning of flue gases turns them into fertilizers for greenhouses and sweep gas, which ensures long-term operation of the membranes and eliminates the need for expensive high-pressure equipment. The profitability of IT OSM technology can be achieved through a combination of new and well-known conjugated technical and logistical solutions which provide a synergy effect for DMG. The success of the pilot project of an eco-estate lies in the two-fold reduction in capital costs and maintenance while meeting modern housing requirements. This result is achieved by a critical selection of compatible solutions, semi-autonomous energy-efficient execution, a combination of passive engineering systems, and a construction roadmap using local resources and wastes. The mass construction of eco-villages with improved quality of housing at a reduced price, together with social and industrial infrastructure, can provide demand for DMG, which can greatly expand the market in the direction of autonomous settlements. A significant part of the conjugated scientific and technical solutions can be useful in other regions and countries.

Keywords

Oxygen selective membranes; composites; cermet; carbon fuels; green coal energy; ecology; sustainable development; eco-settlement; eco-estate

1. Highlights

- Nano-cermet δ-Bi_2O_3/Ag-based IT OSM has the maximum potential for air separation.
- The idea of a smart oxygen membrane will ensure their feasibility.
- Complete combustion of finely ground carbon fuel in oxygen-enriched air.
- Conjugated solutions are effective in the construction of a semi-autonomous eco-estate.
- Distributed multigeneration and eco-villages have synergy and meet modern challenges.
- Rational use of natural resources, sun, and wind energy.

2. Introduction

New eco-settlements on all continents can be seen as sustainable development demonstration projects for mass dissemination with minimal consumption of non-renewable resources and preservation of the environment [1]. In 1995, the Global Ecovillage Network (GEN) was founded. Ecovillages have become a fundamental form of urban implementation of ideas, which are based on local initiatives and the integration of the four dimensions of sustainability: environmental, economic, social, and cultural aspects. GEN began to build interaction between politicians, scientists, entrepreneurs, and eco-communities, implementing a strategy for a global transition to sustainable development. This direction is supported by The United Nations Human Settlements Program (UN-HABITAT) [2]. The program is being updated by existing challenges: such as climate change, the pandemic, and lack of resources. Eco-settlements in different countries are characterized by common features: ecological farming (based on the principles of permaculture), environmental restoration (forest planting), the use of innovative technologies, materials, and alternative energy (windmills and solar panels) [3]. For example, in the Russian Federation, the movement to construct and develop eco-villages began in the 1980s. According to the website [3], more than 200 eco-villages were created with a population of 20,000.

The process of urbanization in Russia, as in other countries, is gaining momentum, but at the same time, there is a positive reverse trend of resettlement to the countryside with urban ideas that maintain a comfortable standard of living, along with new technologies and materials. However, the reverse flow from megacities turned out to be incomparable to the flow of large cities. The pandemic changed the situation a little, but country houses and eco-villages turned out to be just a place for summer residences for those working in megacities. In Moscow and surrounding regions, only 20% of eco-houses were used for winter living. Eco-villages have not turned into stable settlements with schools and other social infrastructure, industrial, and agricultural enterprises that provide residents with income. The main reason for the failure of a promising pilot project is energy. Focusing on alternative non-permanent energy sources (wind and sun) in the harsh climatic conditions required additional permanent sources. The cost of electricity from renewable resources with parameters that are far from the standards turned out to be too expensive with an unlimited Simple Pay-Out Time (SPOT), which is unacceptable for the sustainable development of businesses and eco-villages. The electric energy from gasoline generators is unacceptably expensive for residences and businesses. The provincial electricity network is characterized by low power, voltage variations of 140–240 V, and frequent outages, especially dangerous during severe frosts. This problem is global, bearing in mind that a significant part of the rural population does not have access to a reliable electrical network. Another reason for the slow development of eco-villages is the problem of communications and connection with civilization: road, electrical network to start construction, water and sewerage, heat, Internet, and TV. The direct transfer of urban building technologies to the countryside in a harsh climate led to a high cost per 1 m^2 (2–6 times higher than the modern dwelling of similar comfort in cities like Novosibirsk). Such a difference in prices practically does not give chances for the creation of eco-villages with sustainable development.

The concept of distributed multigeneration DMG, first presented at the 2012 Meeting of ACS in San Diego, CA, fully meets modern challenges, as shown in **Figure 1**. The heart of DMG is a membrane module of intermediate temperature oxygen selective membranes (IT OSM) based on δ-Bi_2O_3/Ag cermet for the separation of oxygen from air at an operation temperature T_o ~ 550°C. The combustion of finely ground and homogenized fuels in an atmosphere of oxygen-enriched air is the main idea of DMG **(Figure 2)**, which ensures complete combustion of carbon with the formation of expensive micro-spherical materials instead of traditional wastes **(Figure 3)**. Environmentally essential complete purification of flue gases turns them into fertilizing for greenhouses and sweep gas, which ensures long-term operation of the membranes and eliminates the need for expensive high-pressure equipment.

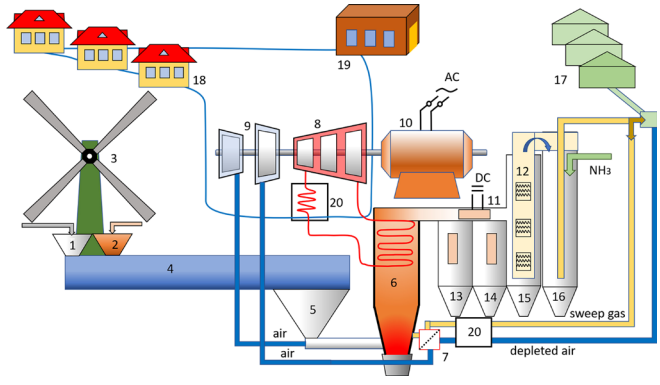

Figure 1: General scheme of DMG. 1 - silo for carbon fuel, 2 - silo for additives, 3 – windmill, 4- ball mill for fine grinding and homogenization, 5 - silo for pulverized fuel, 6 - boiler (reactor), 7 - membrane module for air separation, 8 - steam turbine, 9 - fans, 10 - electric generator, 11 - thermoelectric module, 12 - carbon absorbents in a bag filter for capturing volatile elements, 13-16 - silo for passive coagulation of aerosol particles and precipitation of microspheres fractions, 17 - set of greenhouses with different CO_2 content, 18 - residences and 19 - enterprises with a water heating system, 20 - heat exchangers.

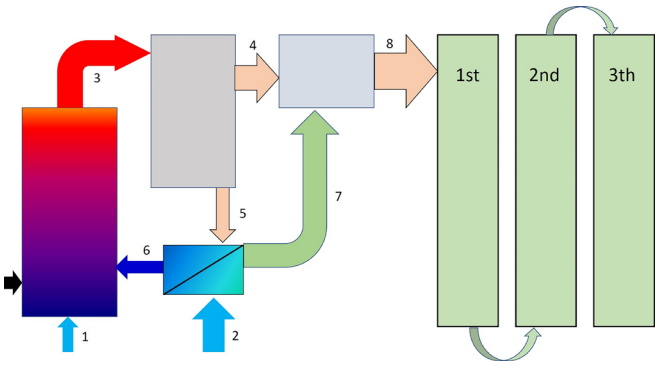

Figure 2: Scheme of gas flows for the case of O_2 enrichment 30% in m-TPP in relative volume units (without Ar): 1 (100 = 79 N_2 + 21 O_2), 2 (1000 = 790 N_2 + 210 O_2), 3 (197.5 = 115 N_2 + 10 O_2 + 68 CO_2 + 4.5 H_2O), 4 (137 = 79 N_2 + 7 O_2 + 48 CO_2 + 3 H_2O), 5 (60.5 = 36 N_2 + 3 O_2 + 20 CO_2 + 1.5 H_2O), 6 (96.5 = 36 N_2 + 39 O_2 + 20 CO_2 + 1.5 H_2O), 7 (964 = 790 N_2 + 174 O_2), 8 (1101 = 869 N_2 + 181 O_2 + 48 CO_2 + 3 H_2O).

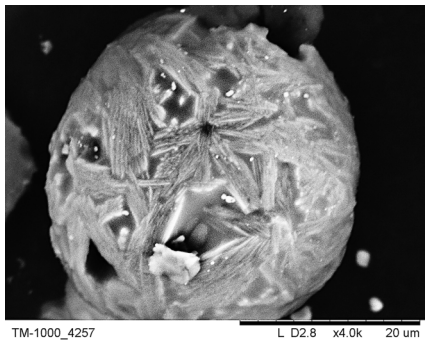

(a)

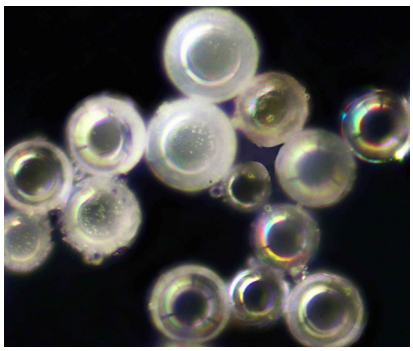

(b)

Figure 3: Ceramic **(a)** and glass **(b)** hollow microspheres.

The optimal power of thermal mini-plants (m-TPP) is 1-10 MW. The potential share of DMG in the electricity market is approximately 7%. This value coincides when assessed from different positions—especially with the volume of the microsphere market for concrete and distributed generation. DMG is in demand primarily in the construction and development of autonomous and semi-autonomous eco-settlements for 100–1000 residences, as illustrated in **Figure 4**.

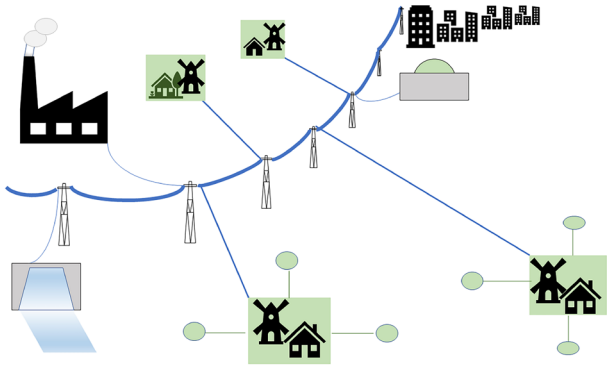

Figure 4: General scheme of an electrical network with low-power lines to ecovillages for their successful construction and sustainable development.

The interest of investors in DMG is directly related to the possibility of mass construction of residences in eco-villages at affordable prices. The successful implementation of the low-cost eco-estate pilot project shows the attractiveness of the process of de-urbanization on a new basis with DMG. Sustainable development with the preservation of the environment and the minimum consumption of non-renewable resources becomes quite evident when creating durable oxygen membranes. The carbon cycle in the eco-settlements with DMG is shown in **Figure 5**. Natural carbon resources are transferred to the soil, and consumers receive energy as well as industrial and agricultural products with the reasonable and efficient use of solar and wind energy.

3. Experimental Part

3.1. Reagents

The precursor materials include Bi_2O_3 (Russia, 99.99% pure), nitrates of REE (former USSR, 99.9% pure), powders of REE oxides (Dy_2O_3, Er_2O_3, China, 99.9% pure), WO_3, Ta_2O_5, Fe_2O_3 (former USSR, 99.9% pure), $HfOCl_2$ (Russia, 99% pure), CuO (Russia, 99.9% pure), Mn_2O_3 (Russia, 99.9% pure), metal powders - Cu (Russia, 99.99% pure), Ag (Russia, 99.9% pure), and Mn (China, 99.9% pure).

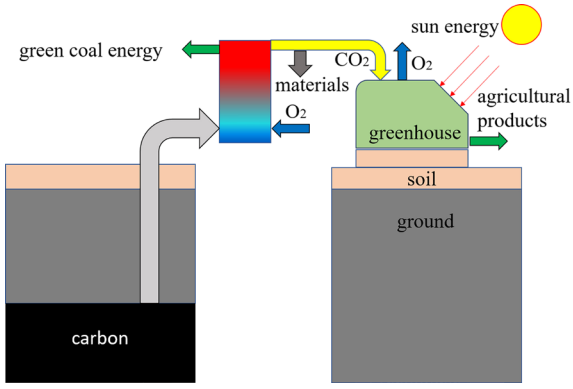

Figure 5: Scheme of the carbon cycle in the ecovillage with DMG.

3.2. Synthesis Techniques

A standard solid-state synthesis route with high-energy ball milling (mechanical activation, MA) in planetary mill AGO-2, Russia was used to obtain all materials. The synthesis of ceramic nano-powders was carried out by a three-step process firing at 800–950°C in the air. Inox steel ball diameter was 4 mm and the ball-to-powder weight ratio ~10:1. Milling time was 5–15 min in the most intensive mode g = 60 (speed of rotation 750 rpm, supplied energy E_s ~ 10–30 MJ/kg). A known technique for ceramic powders was used **[4,5]**, which ensures high powder uniformity and drastically reduced iron contamination of the materials < 0.01 wt%. The technique includes pre-coating the surface of the steel medium with the processed material, continuous processing for 30–60 s, followed by forced mixing of material and balls to avoid the accumulation of material in the dead zone. Mechanical alloying and preparation of metal-matrix composites were done using the same technique. For the study of wettability, submicron particles of Ag were deposited with a density of 1 mg/cm^2 on the surface of ceramic disks from the charged aerosol in Electro-Mass-Classifier (EMC), Nano-powder Technology Ltd, Russia. Coated with silver ceramic discs were subjected to heating up to 600°C in the HT chamber of the XRD diffractometer.

3.3. Samples

A dense ceramic disk with composition $Bi_{0.78}Er_{0.2}Hf_{0.02}O_{1.51}$ (2HESB) was obtained by pressing MA nano-powder at 200 MPa and sintering at 900°C with rapid cooling in air. Ceramic powder samples were obtained with compositions $Bi_{0.78}Dy_{0.12}Er_{0.1}O_{1.50}$ (DE), $Bi_{0.76}Dy_{0.12}Er_{0.1}W_{0.02}O_{1.53}$ (DEW2), $Bi_{0.76}Dy_{0.12}Er_{0.1}Ta_{0.02}O_{1.52}$ (DET2), $Bi_{0.76}Dy_{0.12}Er_{0.1}Hf_{0.02}O_{1.51}$ (DEH2), $Bi_{0.76}Dy_{0.12}Er_{0.1}M_{0.02}O_{1.52}$ (DEM2, for brevity M = mix of Hf^{4+}, Ta^{5+}, W^{6+}). Pressed at 200 MPa, powders were gradually heated up to 600°C with a short exposure of one minute. Spinel $CuMn_2O_4$ and perovskite $La_{0.7}Y_{0.3}Co_{0.5}Fe_{0.3}Mn_{0.2}O_3$ were synthesized from MA powders by firing at 900°C. Alloys with compositions $Ag_{0.7}Cu_{0.3}$ and $CuMn_2$ were obtained by mechanical alloying for the synthesis of metal-matrix composites with spinel and perovskite.

3.4. Characterization

The characterization of samples was carried out through a combination of methods. Powder XRD data at T = 22°C were collected on a D8-Advance (CuKα-radiation), Bruker, Germany. High-temperature XRD studies were carried out at temperatures up to 600°C with the use of HTK 1200N Anton Paar, Austria. The full-profile Rietveld analysis of the powder patterns was done using software PowderCell-2.4 and TOPAS V4.2. A special iterative algorithm was developed with a gradual improvement in the parameters for describing the background and pseudo-Voigt1 (n_a, n_b) profile function. SEM studies with EDS for control of chemical composition were carried out in TM-1000 and 3400N, Hitachi, Japan. The admixture of iron was not fixed, and the content of the introduced dopants did not differ from the initial formulation within the limits of the method error. Electrical conductivity measurements were carried out at T = 140–650°C in isothermal mode using an MNIPI E7-25 immittance meter, Russia, in the frequency range 30 Hz - 1 MHz with standard data processing procedures. Gold electrodes 30 nm thick were deposited on ceramics by sputtering followed by soldering Ag wires.

4. Results and Discussion

4.1. Main Market Sector for DMG

4.1.1. The Main Features of the Implemented Eco-Estate Project in a Harsh Climate

4.1.1.1. General Design and Materials

The original project of a semi-autonomous energy-efficient passive smart eco-estate was implemented by the author in 2017 near the academe township, Novosibirsk, Russia, with the use of new technologies and waste utilization, as stated in **Figures 6** and **7**.

Figure 6: South side of eco-estate in summer.

Figure 7: North side of eco-state in winter.

Novosibirsk is considered the scientific capital of Russia. An initiative comprising scientists aiming for the creation of eco-villages was born in the late 1980s. The author, along with other pioneers, was awarded the 1st prize in an open competition of the Ministry of Construction in 1996 for an eco-house project with the use of local resources. The fly ash processing technology used in the construction was presented at the Leipzig Fair in 1995 and the International Fair in Gdansk in 1998, where it received gold medals in two categories. In more detail, this eco-technology based on the possibilities of EMC techniques is presented in the book **[6]** and papers **[7–9]**. The cost of constructing an eco-house with a living area of 200 m^2, as well as operating costs per 1 m^2 turned out to be 2–3 times lower than in buildings in the academe township. A lot of original and partially patented solutions were implemented in the project. At the same time, several classic solutions for eco-villages were used as well: solar orientation, thermal buffer zones (greenhouse, garage), thermal zoning, maximum use of local resources, a flat roof for growing plants, collecting rainwater for irrigating the site in summer, and permaculture.

The eco-estate is located on a plot of 17 acres. The house was built on heaving ground with a high content of clay minerals up to 45% unsuitable for construction. The water from the well turned out to be unsuitable even for technical needs due to the high content of iron (20-fold excess), manganese, and calcium salts. The temperature 30 km south of Novosibirsk drops to -45°C, and the mean annual temperature ~ -4°C. To deliver building materials, the road 40 m long to the house was made manually with the utilization of local wastes for ground stabilization - fly ash and granite dust **[10]**. The cost of the road was made with a methodology that is seven times cheaper than using a German patent. The foundation without formwork and steel reinforcement in the form of a grillage 0.2 m thick on poured piles with a diameter of 0.15 m, and a depth of 2 m was made of expanded cheap concrete prepared on site with fly ash and cement content of 1:1. The cost of the foundation turned out to be 50 times cheaper than recommended for such ground monolithic Swedish slab. The structure of the matryoshka-type house is made of facing ceramic bricks on the outside and ordinary bricks on the inside, between which there is a wooden frame filled with straw. The calculated coefficient of thermal resistance of multilayer walls with finishing is $R = 6.0$ K·m^2/W, which is two times higher than the requirements of the RF standard. The central massive wall and the inner walls act as load bearing for the steel pipe beams, on which ceilings are made without the involvement of machinery. Beam deflection is minimized as one end of the beams is already fixed. The plinth and the central wall with a width of 1 m at the bottom to 0.6 m at the top are filled with ~55 T ground from the basement. The total mass of the house ~350 T provides a very high thermal inertia with a small load of 0.5 kg/cm^2 on the outer foundation strip, which is most susceptible to external influences. Creating a flat roof with straw insulation, unusual for a harsh climate, turned out to be a cheaper, safer, and faster solution, which is very important due to the short building season. In addition, 1 m of snow on the roof additionally provides negligible heat loss through the roof in winter. The selected flat roof is safe against avalanches and icicles, but it requires snow removal before it begins to melt in early spring. Energy and cost–efficient blind windows eliminate air infiltration. In addition, the windows are equipped with roller shutters on the outside and curtains on the inside to minimize heat losses. The thermos-like houses have no cold bridges and are protected by a heat buffer for half the perimeter.

4.1.1.2. Smart Home Ideas

Home-keeping experience shows that some "smart home" ideas in harsh climatic conditions are not only unprofitable but also dangerous. For example, automatic shutters can jam in the wind or fail after rain and cold snap. The software becomes obsolete too quickly even in comparison with the time of construction. The failure of one of the engineering systems in the house can lead to a domino effect with disastrous consequences. Reducing the voltage in the network in severe frosts to 140–150 V can damage control and UPS equipment. For an eco-house in harsh climatic conditions, cheap passive systems are the most reliable. Some well-known and widely advertised "eco-systems" were not used in the eco-house: For example, 1) solar collectors, despite the high efficiency of modern designs, were not used because the use of water as a heat carrier is impossible due to expansion when frozen. The use of organic liquids is unacceptable due to the high cost, fire hazards, the fragility of rubber gaskets, and chemical reactions with the formation of toxic substances. 2) Solar panels were not used to generate electricity. The system and its installation are very expensive with low durability. When installed on the south wall, the panels reduced the thermal performance of the house. The system is not viable even as a backup system. Efficiency cycles and energy needs are out of phase, requiring an additional energy storage system. As a result, a similar "eco-system" provides the opposite effect. 3) Local treatment systems for wastewater like TOPAS [www/topol-eco.ru] were omitted. Blackwater local treatment is expensive, incomplete, and unreliable in severe frosts.

4.1.1.3. Conjugated Engineering Systems

A modern house for a comfortable family living requires engineering systems, each designed and executed independently in a market economy. The whole combination of modern engineering systems is difficult to combine and install in a short time. In addition, the cost of equipment and installation is too high. The first eco-house project developed by Ecodom Ltd with a compilation of independent engineering systems had an estimated cost that was six times higher per 1 m^2 than a standard apartment in a custom building. The first eco-house in Novosibirsk in a stripped-down version was built in 1998 as a pilot project with the support of the regional government, but it turned out to be unsuccessful and unclaimed. Our successful implementation of the eco-state project was due to the critical selection of solutions offered on the market and the development of passive conjugated engineering systems enabling semi-autonomous execution.

4.1.1.4. Water Supply and Sewerage

The pump in the well periodically supplies water with T = 7°C through corrugated metal pipes to tanks for passive treatment, heated to 9°C in tanks for gray wastewater. The water purification system includes six tanks connected in series with siphons. In the first tank, water is aerated, causing Fe^{2+} ions to oxidize to Fe^{3+} with the formation of insoluble iron hydroxide. Ions Ca^{2+} and Mg^{2+} absorb CO_2 with the formation of poorly soluble calcite $Ca(Mg)CO_3$. Joint coagulation of colloidal particles leads to accelerated precipitation, as shown in **Figures 8** and **9**.

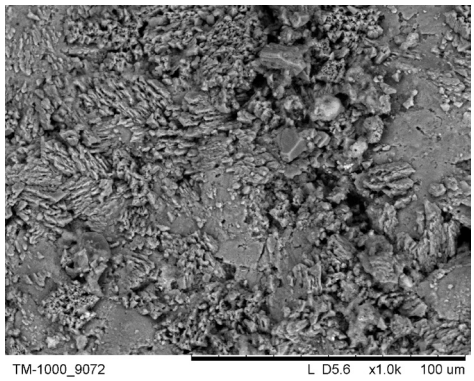

Figure 8: Brown sediment in the 1st tank, content of Fe 1.7, Mn 0.3, Ca 97.7, Mg 0.3 wt%.

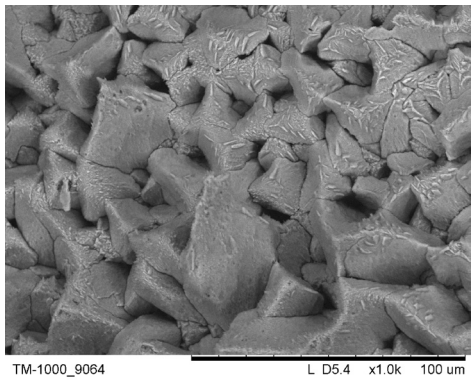

Figure 9: White sediment in the 5th tank, content of Ca 97.9, Mg 2.1 wt%.

After two weeks, purified water with reduced hardness reaches the clean water tank by gravity, from where it is pumped under pressure into the water supply system. In winter, 10 m^3 of water in tanks provides a significant contribution to the thermal inertia of the house, equivalent to 50 T of materials. The implemented passive water supply system practically does not require maintenance. On the contrary, offered on the market complex water treatment systems, based on membrane technology, have not only 5–10 times higher capital costs, but also require constant maintenance, filter changes, and chemicals.

Instead of a custom WC system or Clivus Multrum Composting toilet, 2 semi-dry type bioreactors under the modified toilet bowls are installed in the basement, which is emptied once a year into compost pits. The system consumes 20 times less water than WC. Enriched with nitrogen fertilizers bio-liquid is collected in 20-l canisters and disposed of twice a month on the site. Gray water drains from the kitchen and bath are collected in 10 plastic tanks with a total volume of 7 m^3. In winter, filled water tanks act as a passive heat accumulators. In spring and autumn, gray wastewater is pumped to an underground reservoir at the site to drain into the soil. Market local sewage treatment systems are too expensive (10–20% of the value of the house), require constant maintenance, and are unreliable in winter.

4.1.1.5. Heat System

Due to the good thermal insulation and high thermal inertia of the house, the heating system is based on three sources: expensive electrical energy, relatively cheap energy from a wood-burning water-jacketed fireplace (virtually stored solar energy), and free direct solar radiation through the windows. The heating system depends on electricity, so the house has a backup system of lead batteries to power the circulation pump. The house provides a temperature difference of 5 K per 1 kW of heat energy. At an outdoor T = -30°C, heating power of 10 kW is required to maintain a comfortable temperature of 20°C in the house. Solar radiation provides 0.5 kW, the rest of the heat is supplied by electricity and a fireplace in comparable shares. A heat accumulator in the form of a 200-liter tank with a Na_2SO_4 solution smooths out daily temperature fluctuations. In an open circuit, the heat from the water jacket of the fireplace is transferred by the circulation pump to the accumulator through a corrugated metal pipe. The forced heat distribution system in the house is severely limited due to the high thermal inertia and insulation. The temperature difference between the north and south sides of the house does not exceed 4 K and between floors - 3 K. Electricity is the most expensive heating source, but the choice of a gas heating system makes sense only in the case of access to the gas network at the design stage of the house. Considering the only item of expenditure in the eco-estate for electricity, as a result, the average monthly utility bill is 2–2.5 times less than in ordinary apartments per 1 m^2. Collecting deadwood from forested areas and using it for heating is cheaper and more sustainable, provided that the surrounding forest is cleared of flammable material. Buying firewood in the market provides jobs in the province and sanitary felling in the forest, i.e., maintaining order in the environment. Wood ash in the amount of 200 kg per year is a free potassium fertilizer for the site (market value ~100 USD).

4.1.1.6. Ventilation

A forced ventilation system is required to reduce the CO_2 content in the air according to sanitary standards. A large volume of air in the house, along with indoor plants, allows for meeting the standards without ventilation. However, a simplified ventilation system is installed in the house. From the south side, air is taken at the level of the foundation and is fed into the house by a fan through pipes in the ground. This line is used in summer for ground heating with T ~10°C and passive air conditioning in the house by 3 K. In hot weather with T > 30°C, comfortable conditions are maintained in the house with T < 27°C. On the north side, a similar system is used to ventilate a closed box with bio-reactors and exhausts through a chimney.

4.1.2. Summary

The successful implementation of the pilot eco-estate project is associated with the following solutions: 1) semi-autonomous execution, 2) critical selection of compatible solutions, 3) conjugated passive systems, and 4) use of local resources and wastes for construction and maintenance. Success in the case of the implementation of the first pilot eco-house in a harsh climate on the unsuitable ground shows the prospects of mass construction of semi-autonomous eco-villages with less cost and better execution. DMG will quickly develop this huge market niche and expand to autonomous settlements.

4.2. Oxygen Membranes

4.2.1. Introduction to ITM Technology

The pilot eco-estate project was implemented using a combination of simple compatible solutions. It can be assumed that one of the main reasons for the current general situation in the construction of individual houses is the narrow specialization of business, and earlier in the USSR - the sectoral division of the economy. The failures in energy membrane technology at astronomical R&D costs have the same reason. The creation of oxygen membranes is a complex, but the primarily interdisciplinary task that cannot be solved by traditional division into parts.

4.2.2. State of the Art

The use of Oxygen Selective Membranes (OSM) in the energy sector, in general, is described in the work **[11]**, where estimates of the parameters of oxygen membranes for the viability of Ion-Transporting Membrane (ITM) technology are made. This direction is based on the recognition of the anthropogenic contribution to global warming due to CO_2 greenhouse gas emissions. The three main routes for mitigation of CO_2 emissions in electricity plants were defined as follows:

1. Post-combustion processes: CO_2 is captured from the flue gases.

2. Pre-combustion processes: The fuel (natural gas or coal) is converted into hydrogen and CO_2. The CO_2 is separated, and hydrogen is combusted in a gas turbine.

3. Oxyfuel processes: Combustion is carried out using pure oxygen, resulting in a flue gas that mainly contains water (H_2O) and CO_2.

The authors also carried out economic evaluations of processes based on tubular self-supporting membranes at an oxygen flow of 10 ml/cm^{2}min **[11]**. Well-known mixed ion-electron conductive (MIEC) LSCF and BSCF perovskites provide such oxygen flow at high temperatures T ~ 1000°C. For economic viability, SPOT should be smaller than five years, but estimates gave 17 and 11 years for large and small-scale systems respectively. The calculations were made on the assumption that on the supply side the partial pressure of oxygen is 1 bar, and the fuel of the synthesis gas type is used as the sweep gas. This gap can be reduced by several factors: cheaper membranes, higher flux through the membranes, longer lifetime of the membranes, higher energy prices, and CO_2 trading. Fluxes will have to be at least two to three times higher if this were the only option. However, over 40 years of MIEC perovskites research, their compositions have been optimized along with other aspects. CO_2 trading remains the only tool to maintain the viability of ITM technology for the energy sector.

4.2.3. Global Warming and Related Phenomena

The hypothesis of anthropogenic contribution to global warming is not substantiated in the usual manner using independent experts. Moreover, global warming advocates confuse completely different concepts, global warming, climate change, and ecology. There is only one reliably established fact of an increase in the content of CO_2 in the atmosphere in recent decades from 300 to 400 ppm. According to the study of Antarctic ice **[12]**, the increase in the concentration of CO_2 in the atmosphere in the last 800,000 years was due to warming, which is subject to the Milankovitch cosmic cycles.

The main absorbent of CO_2 is the ocean. The relatively rapid increase in atmospheric CO_2 concentration in recent decades has been due to slow absorption by ocean and vegetation. The ocean absorbs CO_2 more slowly due to the decrease in pH of seawater. The acidification of seawater is caused by the absorption of SO_x and NO_x acid gases from the atmosphere. The peak emission of acid gases in coal-fired generation in 2000 was 210 million TPY, and the total emission of CO_2 was about 40,000 million TPY **[13]**. In mass terms, CO_2 is about 200 times more. However, the acidity of SO_x and NO_x is 5 or more orders of magnitude higher than that of CO_2. The contribution of CO_2 to ocean acidification is negligible (less than 1%) for any model of the dynamics of SO_x and NO_x oxidation. The emission of SO_x and NO_x in the 1980s led to noticeable changes on land, such as the destruction of structures, the oppression of many types of vegetation and living organisms, the increase in the acidity of the world's oceans, and other visible consequences like the death and oppression of coral reefs. Legislation to reduce SO_x and NO_x emissions has been adopted in many countries around the world, resulting in overall reductions in emissions. The most negative effect of acid rain is that acids accumulate in the ocean since there are no insoluble sea salts of sulfates and nitrates. Some algae can absorb S- and N-contained compounds more than others. It is a strong and abrupt intervention in the ocean ecosystem with negative results that will continue until a new equilibrium is established.

4.2.4. Emission of Greenhouse and Acid Gases

CO_2, water vapor H_2O, and CH_4 are greenhouse gases. An increase in CO_2 content in the atmosphere unequivocally increases the yield of agricultural production. The negative impact of CO_2 on the climate and ecology requires irrefutable evidence. Instead, several countries and organizations have decided to move to a carbon-free economy. This means a ban on coal energy and a focus on renewable energy sources (sun, wind, and hydropower). With a real shortage of conventional energy resources approaching, there is a real need to attract more renewable resources and reduce environmental problems. Coal combustion is indeed the main source of industrial solid wastes, which is located near most of the world's population. Solid wastes in the form of ash and slag contribute to the pollution of water sources and soil due to leaching **[14]**. However, the greatest harm to the global environment is caused by the emission into the atmosphere, together with the exhaust gases, of acid oxides SO_x and NO_x, volatile elements (Hg, As, etc), particulate matter, and aromatic organic compounds **[6,8]**. Restrictions in coal energy due to CO_2 emissions look at least unreasonable. A

carbon-free economy and additional taxes for the carbon footprint require justification since it is known that the potential for CO_2 natural emission from permafrost is 1670 billion tons, while industrial emissions are only 8 billion tons [15]. Decarbonization of the economy is an unreasonable, expensive, and senseless program. Not to mention that The United Nations Human Settlements Program (UN-HABITAT) considers climate change [16]. Indeed, quite recently, about 3–6 thousand years ago, mammoths and tigers lived in the zone of today's permafrost zone.

4.2.5. Errors in Mean Temperature Calculations

Concerning global warming, when industrial growth was observed, estimates of mean land temperature usage data from weather stations show a slight increase in *T* at a noise level of 1–2 K in recent decades. However, the validity of using these data for climate assessments is highly questionable because there are at least three sources of systematic errors with a plus sign.

1) Weather stations are located very unevenly around the planet, but mainly in the places of residence of the population, and are intended for weather forecasts for several days. The inevitable heat contamination noticeably increases the local temperature. For example, the mean winter temperature in our site with an eco-estate is 3–5 K lower than in a city 30 km away.

2) In the largest country in the world, the USSR, from 1987 to 1989, the number of weather stations decreased by 15%. At the beginning of 1995, the decrease in the number was 22%. At the same time, the stations were closed in remote regions with cold climates, which happened in other places not only in Russia.

3) The share of the land on the planet is ~ 29%. If 18,000 years ago the level of the world's oceans was 110 m lower, then the coastline was much further than it is now. The air temperature near the coastline is higher than inland. Therefore, the approach of the ocean to weather stations increases measured *T*.

Moreover, an increase in the water surface on Earth leads to an increase in mean humidity and thus to an increase in the content of the main greenhouse gas. Measurements of the mean CO_2 content in the atmosphere in ppm units are not difficult, and the data obtained are reliable and reproducible. On the contrary, it is extremely difficult to record the change in the content of water vapor against the background of their high content and strong *P-T* dependence.

4.2.6. CO_2 Capture and Storage

The primitive argumentation of global warming by anthropogenic emissions of greenhouse gases is disproportionate to the proposed measures to create a carbon-free economy. In a paper by Congress Budget Office [17], the range of cost estimates for CO_2 capture and storage is presented for different power plants and geo-structures. The mean cost of CO_2 capture and storage is about ~50 USD/T. In such a case, burning 1 T of coal with a carbon content of 80% will result in 3 T of CO_2. The cost of coal in 2009–2019 averaged 90 USD/T [18] and the cost of CO_2 capture and storage was 150 USD/T. When CO_2 is captured and stored, coal generation of electricity becomes meaningless. There are also doubts about the correctness of estimates of the cost of CO_2 capture since residual acid gases quickly destroy expensive compressor equipment.

Risks of CO_2 storage in underground geo-structures and oceans are underestimated. In the event of a leak, which can occur due to geological processes in the earth's crust, CO_2 collects in the lowlands and can lead to disaster. The violent potential for such CO_2 disposal became clear in August 1986, when Lake Nyos in Cameroon erupted with a blast that some locals mistook for the testing of a nuclear weapon. As much as 1 cubic kilometer of heavier-than-air CO_2 flooded low-lying regions, suffocating more than 1,700 people [19].

4.2.7. OSM Based on δ-Bi_2O_3/Ag Cermet

4.2.7.1. History of Cermet Membranes

Based on cermet OSM from the best oxygen-ion δ-Bi_2O_3 and electronic Ag conductors have maximum air separation potential at intermediate temperatures. These cermets were first studied in the works [20–23]. The published studies of the two groups were carried out on thick polished ceramic discs with $Bi_{0.8}Er_{0.2}O_{1.5}$ (ESB) solid electrolytes. The Fluorite of this composition has high oxygen-ion conductivity, but the structure remains only for a few hours. Dense cermet samples with grain sizes of approximately 5–10 μm were obtained by the standard ceramic method with high-temperature sintering. A stable interpenetrating cermet structure was obtained only at a silver content of ~ 40 wt%, which greatly exceeds the percolation threshold. The obtained samples showed low permeability because the process was limited by the surface exchange reaction of oxygen at the contact line of gas, solid electrolyte, and silver. In addition, it was even concluded that the use of cermet membranes is fundamentally impossible due to their degradation [23]. In our work, it was also shown [24] that the preparation of dense nano-cermets by hot pressing with a grain size of ~ 50 nm from nano-powders of mechanochemical origin leads to rapid total degradation, even at low temperatures instead of the expected sharp improvement in properties. The total degradation of nano-cermets includes phase degradation of a solid electrolyte with a fluorite structure, recrystallization, segregation of silver on the inner and outer surfaces of the cermet, and disappearance of the interpenetrating structure of the composite with loss of functional properties.

4.2.7.2. Areas of Our Studies

An analysis of a large amount of our data on the rapid degradation of nano-cermets of mechanochemical origin made it possible to link the cause of accelerated degradation with the specific features of mechanochemical powders. According to the theory of ultrafast mechanochemical synthesis in a binary mixture of oxide powders, which also describes the phenomenon of Mechanical Activation (MA) in the case of a single compound, high-energy ball milling at a loading intensity above the threshold leads to the formation of a dynamic state (*D*)* on the contacts of particles in the form of rollers from an atomic mixture of reagents. Relaxation of the dynamic state after loading under quenching conditions leads to the formation of products with a huge free volume of about 10%. Direct measurements by Mössbauer spectroscopy, He

pycnometry, as well as by studying the shrinkage of powders showed a free volume of ~9% [25].

Our research includes the following:

1) Study of the mechanism of phase transformations in metastable fluorite δ-Bi_2O_3;

2) New compositions of compatible materials: solid electrolyte, electronic conductor, silver fillers, modified steel substrate, ceramic filler for substrate, and protective layer and catalyst for exchange reactions;

3) A new multilayer architecture of thin flexible membranes on a substrate;

4) New multilevel nanocomposites with a controlled interpenetrating and core-shell structure from compatible materials;

5) A smart oxygen membrane that provides a technically feasible transition from raw components to an operating membrane with an optimal architecture for energy applications with accommodation at all stages of the life cycle: fabrication of green membranes from specially developed materials under mild conditions without high-temperature sintering with inevitable shrinkage mismatch, preparation of membranes for operation with the formation of a selective layer, and operation mode with periodic fast regeneration.

4.2.7.3. Advantages and Issues of OSM Based on Cermet δ-Bi_2O_3/Ag

Against the general background of failures in the development of ITM technology based on MIEC perovskites, the number of works on cermet membranes is disproportionately small. The research ended at the first stage of primitive disks. We believe that the creation of real OSM with sufficient durability is possible only as a result of understanding all the processes occurring in the system, including primarily the degradation. Optimism in the development and implementation of OSM in the energy sector has serious grounds. Indeed, the requirements of the DMG for membranes are incomparably softer than in the case of the traditional approach – oxy-fuel combustion in pure oxygen [11]. **Table 1** and the issue sheet below represent our understanding of OSM to date [25–28].

The presented factors are interrelated and conjugated with each other. This once again proves that the complex task of creating a viable membrane cannot be solved by simple separation into parts.

Table 1: Advantages of OSM based on cermet δ-Bi_2O_3/Ag compared to perovskite membranes [11].

Option/property	cermet	MIEC perovskites
Operation temperature	~550	>800
Oxygen-ion conductivity	highest	lower by 1-2 orders
Electronic conductivity	highest	lower by 4-6 orders
Catalytic activity	medium	weak
Mechanic	flexible	brittle
Thickness of selective layer	10-20 μm	10-40 μm
Support	modified inox steel mesh	porous perovskite ceramics
Form	flat	tubular
Module assembly	simple	complex
Steel piping of membrane modules	cheep	~ 50% of the module cost

Apparent Issues of OSM Based on Cermet δ-Bi_2O_3/Ag:

A. Metastable phase of disordered fluorite at $T < 730$°C;
B. Recrystallization and segregation of silver;
C. High permeability is achievable only in nano-cermet;
D. Nanomaterials are thermodynamically unstable;
E. Formation of free volume in ceramics during high-energy ball milling;
F. Chemical reactivity of Bi_2O_3;
G. *P-T* conditions of consolidation of the gas-tight selective layer are unacceptable for commercialization.

4.2.7.4. Phase Degradation of Metastable Disordered Fluorite δ-Bi_2O_3 (A+C+D+E)

The problem of phase degradation at low temperatures of disordered fluorite δ-Bi_2O_3, which is stable at $T > 730$°C, has long been known. According to XRD, when the phase changes are not yet noticeable, the deterioration of the conductive properties is already very significant [29].

At the same time, changes in the structure were observed by neutron [30] and electron diffraction [31]. We studied the mechanism of initial structural changes in dense fluorite ceramics by in situ HT XRD and found that the first stage of phase degradation begins on the surface without the formation of nuclei by the mechanism of spinodal decomposition [28]. The fluorite structure is elongated along the 111 axis due to the ordering of oxygen vacancies with the formation of a rhombohedral phase, S.G. *R*-3 [28,32]. At the initial stage, the process proceeds instantaneously for surface crystallites with the 111 faces oriented parallel to the surface. For surface crystallites with other orientations, the deformation process is slowed down, while for bulk crystallites, the kinetics is described by a root dependence on time, which indicates the influence of cationic diffusion—shown in **Figure 10**.

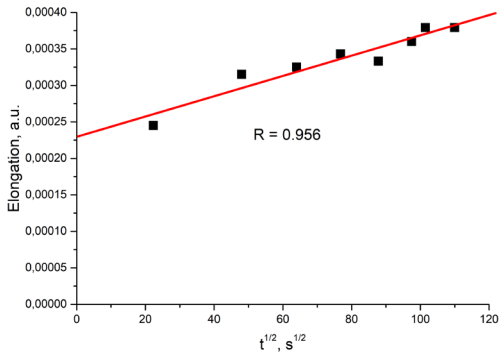

Figure 10: Root time dependence of elongation along <111> axes of fluorite $Bi_{0.78}Er_{0.20}Hf_{0.02}O_{1.51}$ (2HESB) during annealing at 600 °C [25].

Mechanical stresses caused by the phase transformation of fluorite into a rhombohedral phase gradually relax through intergranular cationic diffusion. The process of ordering oxygen vacancies is reversible. Heating up to 640–700°C leads to complete and fast regeneration of the fluorite structure [28]. However, the inevitable changes in the morphology of the ceramic surface persist, as shown in **Figure 11**.

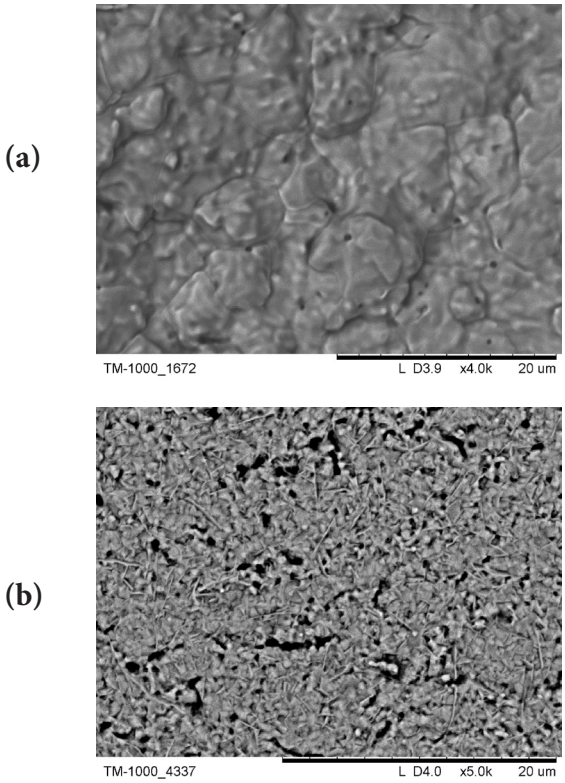

Figure 11: SEM images of 2HESB ceramics before **(a)** and after **(b)** annealing at 600°C and rapid regeneration at 700°C [25].

With long exposure, the metastable fluorite gradually transforms into various stable phases depending on the composition: evident in the rhombohedral phase (S.G. *R*-3*m*), tetragonal phase consisting of fluorite-like layers linked by tetrahedra $Hf^{4+}O_4$, or other cations of medium and small size such as Fe^{3+} (S.G. *P*-4), cubic sillenite with small cations in 2*a* site (S.G. *I*23), which is shown in **Figure 12 [28,33]**.

The regeneration of fluorite structure is possible by heating up to 820°C. However, such an operation is unacceptable for membranes since irreversible significant changes in the microstructure and architecture will lead to a deterioration of functional properties. For targeted inhibition of the ordering of oxygen vacancies and phase transformation into stable phases and different minor dopants of δ-Bi_2O_3 are required [28]. To inhibit the ordering of oxygen vacancies without significant deterioration of conducting properties, it is necessary to use small additions of highly charged cations like W^{6+} to the composition, mainly stabilized by dopants with high polarizability (Dy^{3+}, Er^{3+}). To inhibit the transition to stable phases, a composition of dopants is required that ensures equidistance from all three phases, as shown in **Figure 12**. This can be achieved by optimizing the composition of the minor dopants and better homogenization of the fluorite to avoid nucleation. Fine-tuning of minor doping is in progress. However, the best composition in terms of phase stability relative to HESB has already been obtained while maintaining the conductive properties [28]. Note that the search is based on the principles of high-entropy ceramics and low diffusion activity of minor dopants.

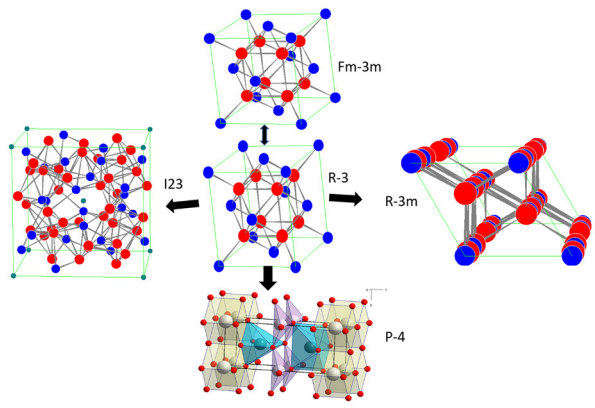

Figure 12: Phase transformations of δ-Bi_2O_3.

4.2.7.5. Recrystallization and Segregation of Silver (B+C+D+G)

Silver segregation is the second most important problem in cermet membranes. Sintering and recrystallization of nanoceramics in cermet during long-term operation of the membrane is inevitable at T ~ 500–600°C. Silver is a very plastic metal with a relatively low melting point T_m = 962°C. In such a case, silver with its high activity in recrystallization is additionally subjected to mechanical pressure with inevitable segregation on the inner and outer surfaces of the cermet, as shown in **Figures 13** and **14**.

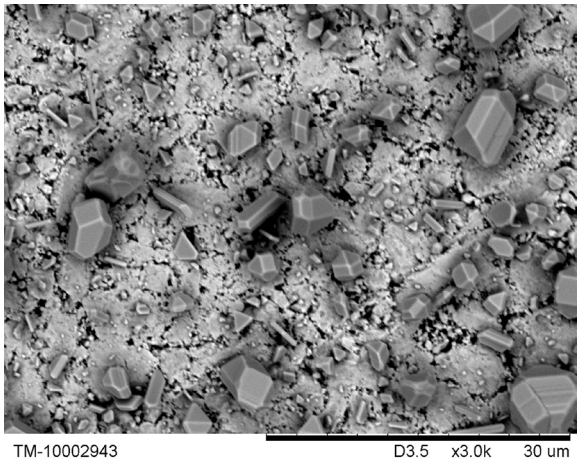

Figure 13: SEM image of Ag crystals in cermets 60F/40(Ag@$LaCrO_3$) **(a)** and 60F/40(Ag@$La_{0.5}Y_{0.3}Pr_{0.2}Cr_{0.5}Fe_{0.3}Mn_{0.2}O_3$) **(b)** after testing 500 h at 500°C (F = $Bi_{0.76}Y_{0.06}Er_{0.08}Tb_{0.08}W_{0.02}O_{1.5+x}$).

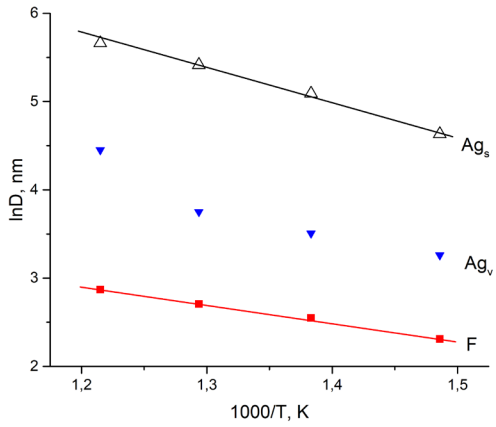

Figure 14: Arrhenius plot of grain size according to full profile analysis on the annealing temperature for cermet 60F/40Ag, F = $Bi_{0.75}Er_{0.23}Pr_{0.02}O_{1.5+x}$, surface Ag_s and volume Ag_v.

To preserve the cermet nanostructure and prevent silver segregation, we proposed the use of an Ag core-shell nanocomposite as an electronic conductor as an alternative, where ceramic fillers will act as the core **[34]**. Such a metal-matrix composite with a rigid ceramic framework inhibits the processes of recrystallization and segregation in the case of good wettability of the components **(Figure 13)**. The wetting theory between solids is absent, so the search for the optimal filler with good wettability of silver lasted about ten years. First, a weak correlation was found for the decrease in silver segregation in the insulator, semiconductor, and conductor series. Testing of a mixed conductor $Bi_{0.8}La_{0.2}MnO_3$ with high oxygen activity **[35]** as a silver filler showed maximum segregation. At the next stage, perovskites with high electronic conductivity based on $LaCrO_3$ were tested as silver fillers, which confirmed the correct direction of the search, as shown in **Figure 13**. After that, several materials with a relatively small variation in conductivity were synthesized with perovskite and $CuMn_2O_4$ spinel structure **[25]**. To quantitatively compare the wettability of silver with the best materials found **[25,34]**, submicron silver particles were deposited from a charged aerosol on porous ceramics **[9]**, which is shown in **Figures 15–17**.

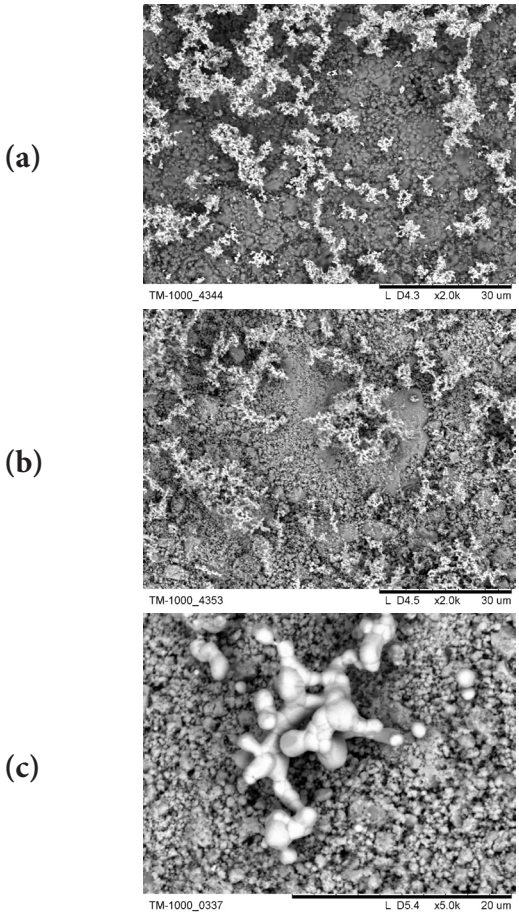

Figure 15: SEM images of spinel $CuMn_2O_4$ **(a)** and perovskite $La_{0.7}Y_{0.3}Co_{0.5}Fe_{0.3}Mn_{0.2}O_3$ **(b-c)** with deposited Ag particles, **(c)** after annealing at 500°C.

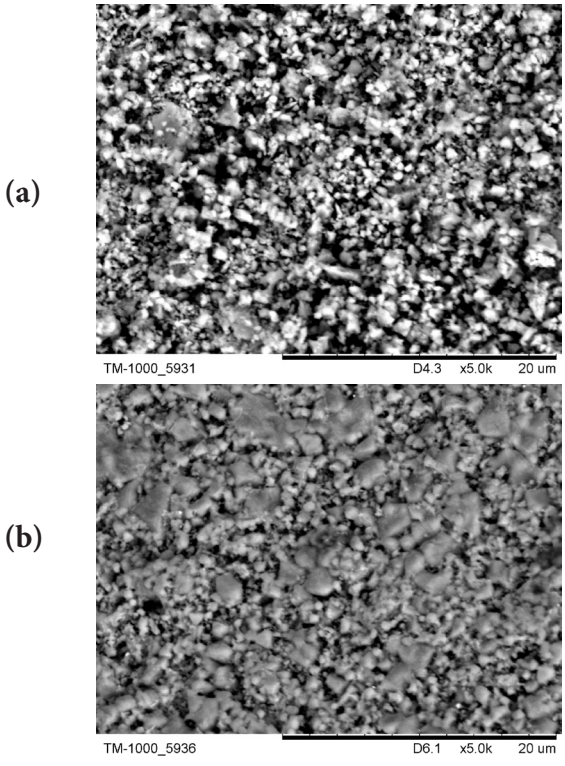

Figure 16:(a) SEM images of spinel $CuMn_2O_4$ back side **(b)** and with deposited Ag particles after one-hour annealing at 500°C.

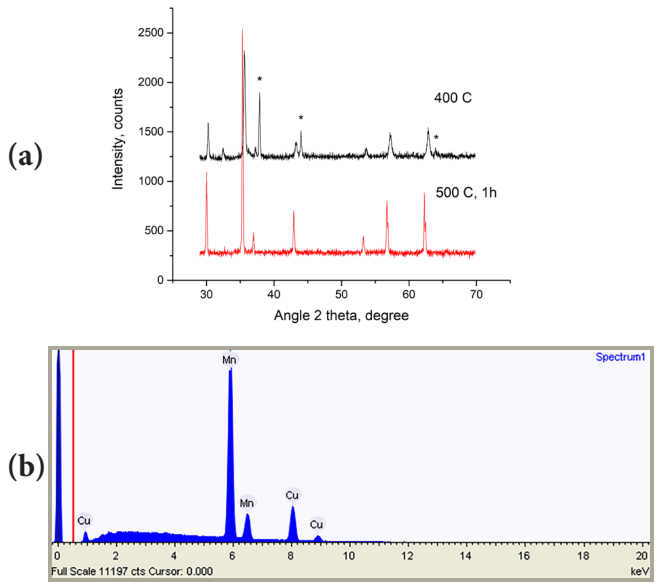

Figure 17: (a) HT XRD (top, *- peaks of Ag) and **(b)** EDS of $CuMn_2O_4$ ceramic disks with deposited Ag particles after annealing for one hour at 500°C.

Annealing in situ experiments by HT XRD made it possible to obtain the kinetics of the decrease in relative intensity of the main Ag peak (reverse wettability $W^{-1} = I_{Ag}/I_{cer}$ in perovskites and spinel). The data obtained unambiguously confirmed that the wettability of silver correlates with the electronic conductivity of ceramics, as illustrated in **Figure 18**. The spinel ceramics at 500°C completely absorbed silver into the volume of the ceramic, so Ag was not detected by XRD and EDS, which is shown in **Figure 17**. Moreover, silver promoted the sintering of spinel, as shown in **Figure 16**. The dramatically improved wettability of silver by spinel as compared to perovskites should have an additional factor in conductivity. Close lattice parameters of spinel ($a/2$ = 4.16 Å) and silver (a = 4.09 Å) indicate possible topotaxy, described in **Figure 19**. Moreover, silver is actually a solid solution of oxygen in the Ag-matrix **[36]**. The perovskite structure with O-O distance ~ 2.75 Å has no structural correspondence with silver.

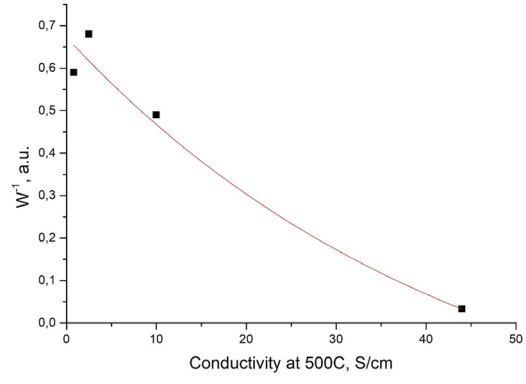

Figure 18: Dependence of the reverse wettability on the electronic conductivity of ceramics.

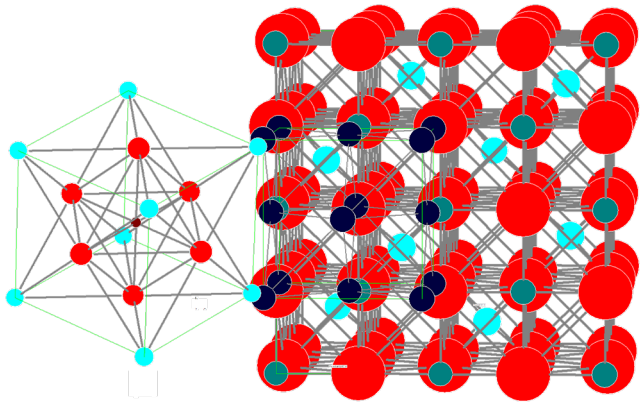

Figure 19: Comparison of structures of perovskite (left) and spinel with silver (dark balls).

4.2.7.6. Interaction of δ-Bi_2O_3 with Ag (E+F)

The very idea of cermet of δ-Bi_2O_3/Ag is based on the absence of any chemical interaction between the components. In fact, silver is a solid solution of oxygen in the fcc lattice with Ag_2O clusters on the surface. This feature of silver has been known since the 19th century and is widely used in medicine, pharmacology, catalysis, and other fields **[37,38]**. The chemical reaction of δ-Bi_2O_3 with Ag *a priori* has a very low rate because the concentration of Schottky defects in the crystal structure $n/N \sim \exp(-\Delta E/kT)$ is usually $\sim 10^{-5}$. In addition, the ionic radius of Ag^+ is much larger than that of Bi^{3+} (1.15 and 1.03 Å respectively for CN = 6). The incorporation of Ag^+ into the fluorite lattice looks unlikely, so the process has not been studied. However, in nano-powders of a mechanochemical origin, the free volume (vacancy defects) in the lattice is $\sim 10^{-1}$ according to the theory and experimental results **[39–41]**. Thus, high-energy ball milling, in addition to the possible direct mechanochemical interaction, accelerates thousands of times thermally activated chemical interaction of Ag_2O surface clusters with bismuth oxide. In this case, the incorporation of Ag^+ into the fluorite lattice becomes possible to observe by the powder XRD method, shown in **Figure 20**. Arrow 1 shows the result of mechanochemical synthesis, 2 the annealing of free volume, and 3 the thermally activated chemical reaction.

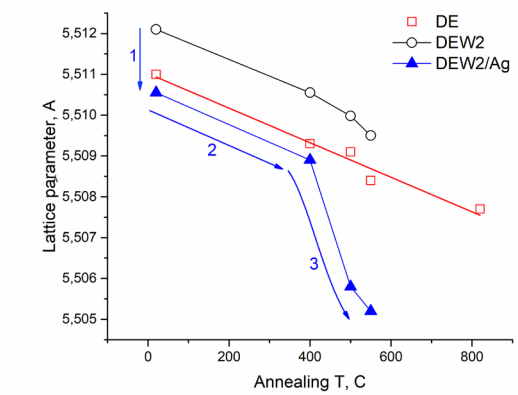

Figure 20: Dependence of fluorite lattice parameter on the annealing temperature. Nanocomposite DEW2 + 10 wt% Ag after 10 min MA.

4.2.7.7. Interaction of δ-Bi_2O_3 with Pd, Pt (A+D+E+F)

In very thin membranes, surface exchange reactions limit oxygen permeability. Noble metals are known catalysts for exchange reactions. A strong influence of Pd on the recrystallization and segregation of silver was studied in our works **[24,27]**, but chemical interaction was not observed, which is shown in **Figure 21**.

The dramatic effect of Pt on the phase composition of fluorite ceramics with similar compositions after calcining for one hour at 600°C is shown in **Figures 22–24**. In the DE ceramics stabilized without minor highly charged dopants, fluorite transforms into a tetragonal phase, rhombohedral phase, and fluorite with a small lattice parameter (a = 5.173 Å) close to Bi_2O_4 **[42]**. These results clearly indicate the oxidation of Bi^{3+} to Bi^{5+} in direct contact of Pt with fluorite. In the 2HESB sample, which is positioned as the most stable and conductive ceramics **[43]**, the initial fluorite (a = 5.505 Å) practically disappears, transforming into fluorite with a small lattice parameter, sillenite, and a tetragonal phase. All three phases are formed due to the appearance of Bi^{5+} ions in a noticeable amount. The least significant changes are observed in the DEW2 ceramics with an increased oxygen content, shown in **Figures 24** and **25**.

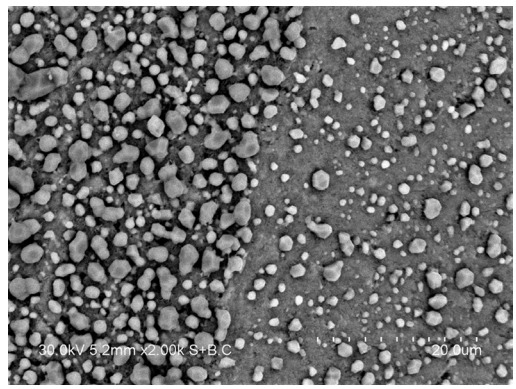

Figure 21: SEM image of Ag crystals in original (right) and modified by Pd (left) surface of cermet Ag/$Bi_{0.76}Er_{0.22}Pr_{0.02}O_{1.51}$ after annealing at 650°C.

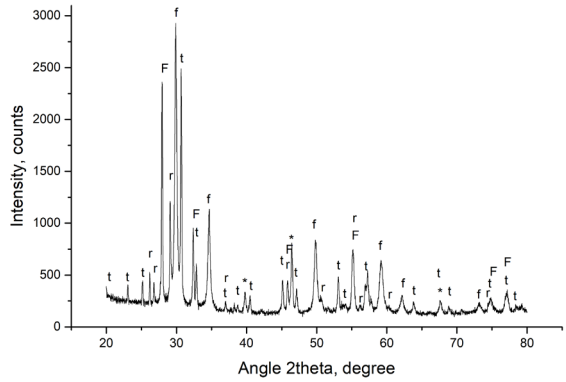

Figure 22: XRD pattern of ceramic disk DE with deposited Pt after annealing at 600°C. F- original DE fluorite with a = 5.524 Å (a = 5.511 Å before annealing with Pt), f- fluorite with a = 5.173 Å, t- tetragonal phase (S.G. *P*-4), r- rhombohedral phase (S.G. *R*-32/*m*), *- catalyst Pt.

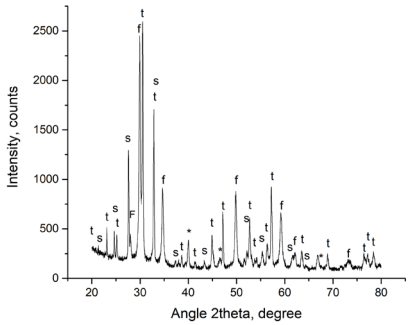

Figure 23: XRD pattern of ceramic disk 2HESB with deposited Pt after annealing at 600°C. F- original fluorite with a = 5.505 Å, f- fluorite with a = 5.173 Å, t- tetragonal phase, s- sillenite, *- catalyst Pt.

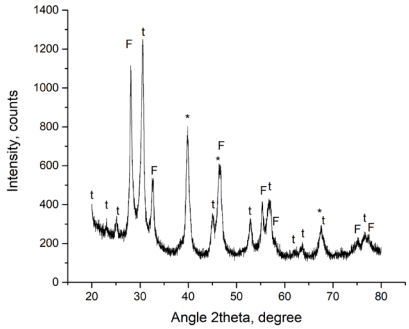

Figure 24: XRD pattern of ceramic disk DEW2 with deposited Pt after annealing at 600°C. F- fluorite, t- tetragonal phase, *- catalyst Pt.

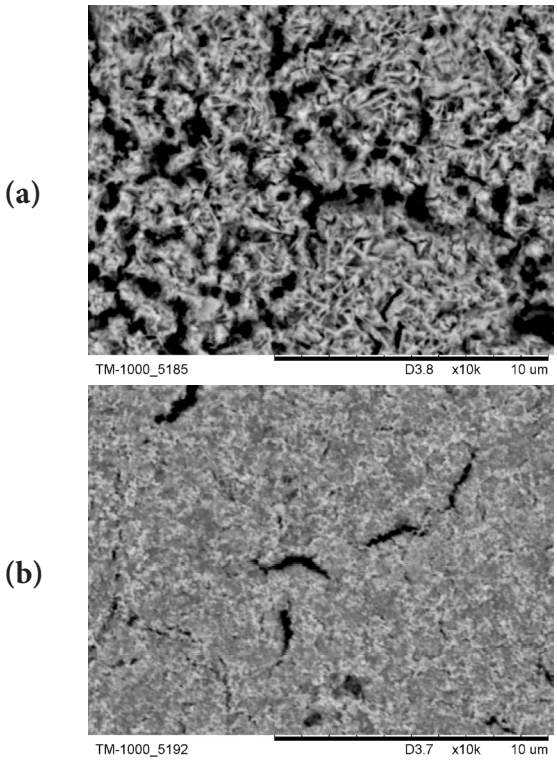

Figure 25: SEM images of ceramics 2HESB **(a)** and DEW2 **(b)** with deposited Pt after annealing at 600°C.

The formation of the tetragonal phase can be attributed to the appearance of Bi^{5+} cations, since annealing without platinum leads to the formation of sillenite, as shown in **Figure 26**.

The unique oxidizing ability of platinum is probably associated with Pt(Bi)O-clusters [**44**,**45**]. Note that platinum inclusions are always observed during the growth of sillenite crystals in Pt vessels **[46]**. The formation of clusters can explain all the observed results, shown in **Figures 22–25**, including strong change in ceramic morphology and Pt crystal formation at 600°C, i.e., at an unusually low T = 0.428 T_m, shown in **Figure 27**. The presence of bismuth in the catalyst not only improves the dissociation of molecular oxygen **[35]** but also increases the mobility of platinum atoms. The deposition of Pt electrodes was a common procedure for measuring conductivity in δ-Bi_2O_3 **[47]**, but it was measured by us: it was one order of magnitude lower than with gold electrodes due to total degradation.

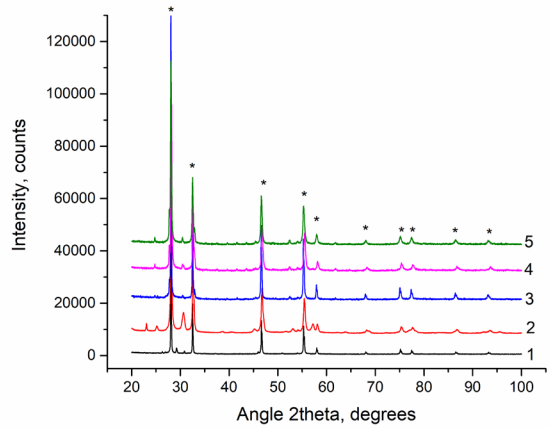

Figure 26: RT powder XRD patterns of MA powder pressed disks after heating up to 600 °C. *- peaks of fluorite, 1- DE (+ peaks of rhombohedral phase, S.G. R-3m), 2- DEH2 (+ peaks of tetragonal phase, S.G. P-4), 3- DEM2 (+ peaks of sillenite), 4- DET2 (+ peaks of sillenite), 5- DEW2 (+ peaks of sillenite).

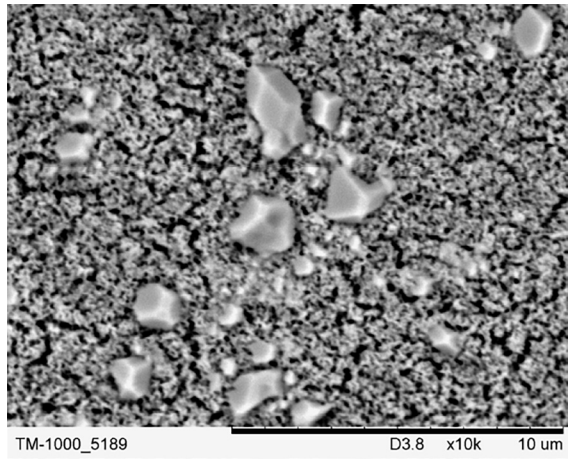

Figure 27: SEM image of Pt crystals on the surface of 2HESB ceramics after annealing at 600°C.

Pt(Pd) alloy with a synergy effect as a catalyst was planned to be used in thin oxygen membranes [26,27]. A sharp boundary between the modified and original regions in Figure 21 indicates a small distance ≤ 2 μm for the spillover effect. The obtained results confirm the need to create a thin protective porous layer between the catalyst and the selective layer in the membrane architecture to activate only spillover and jump-over effects in O_2 dissociation without oxidation of Bi^{3+} and activation of bismuth mobility [26,34]. Moreover, the obtained results show the prospects of a Pt(Pd) catalyst with bismuth additives, including the increase of the oxygen activity and reduction of the cost of the catalyst, but this still maintains the risk of noble metal spreading.

4.2.7.8. Interaction of δ-Bi_2O_3 with Ceramic Fillers (A+E+F)

In the operating membrane architecture (Figure 28), bismuth oxide is in contact with ceramic fillers of Ag-alloy and substrate, and a protective layer as well. Long-time contact of δ-Bi_2O_3 at T_o with ceramic phases containing small cations (Fe^{3+}, Co^{3+}, etc) should lead to interdiffusion with subsequent phase degradation of fluorite to a tetragonal phase or sillenite. Study of this process and optimization of chemically compatible with Bi_2O_3 ceramic fillers are in progress.

4.2.7.9. Preparation of Nano-Powders (D+E+F+G)

Synthesis of nano-powders of membrane components, especially composites, requires the use of mechanical treatment. The grinding and mixing of powders are inevitably accompanied by contamination with materials of balls and jars. Usually, steel or agate balls are used in laboratory mills. Impurities like Fe^{3+} and Si^{4+} are most undesirable for δ-Bi_2O_3, even at the ppm level, since they promote the nucleation of stable tetragonal phase and sillenite. It can be assumed that the most suitable material for jars is YSZ ceramics and HfO_2 for balls due to their high wear resistance and density. To produce nanocomposites, high-energy ball milling is practically the best technique when using nano-powders separation [48]. With such processing of nanomaterials, mechanochemical phenomena inevitably appear; therefore, the approach is called the Mechanochemical Ceramic Method (MCM) [40]. A semi-quantitative theory of ultrafast mechanochemical synthesis of complex oxides was developed in the 1990s [39]. The main provisions of the theory include the threshold nature of the interaction with the roller mechanism of mass transfer and the formation of compounds that have a huge free volume and belong to tolerant structural types. These provisions are also valid in the particular case of single-phase systems [40]. Mechanochemical nano-powders have a stable hierarchical structure: Nano-crystallites less than 100 nm with a free volume of up to 10%, aggregates with sizes < 2 μm and relative density *RD* ~ 0.80, and secondary agglomerates with sizes up to 100 μm and *RD* ~ 0.70 [9,40]. For the separation of agglomerated nano-powders, a new class of eco-engineering EMC was developed [7–9]. The operating principle of the EMC is based on the generation of charged aerosols (gas-dusty plasma) and separation in external fields [7]. To obtain functional materials with better characteristics, the presence of free volume and other specific features of mechanochemical nano-powders are usually of negative importance. However, by eliminating the features, nano-ceramics of high quality can be obtained (fluorite δ-Bi_2O_3 in Figure 29).

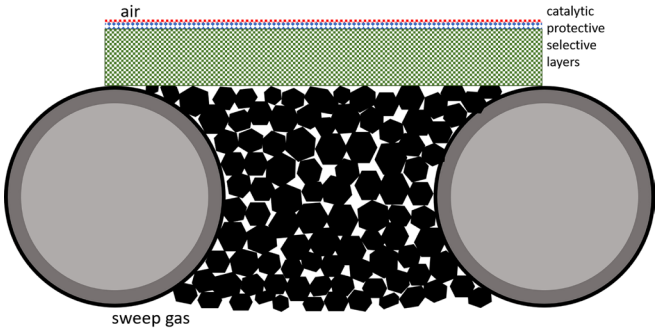

Figure 28: Operating membrane architecture.

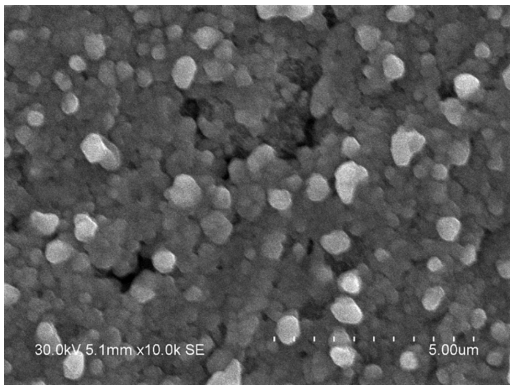

Figure 29: SEM image of a cleavage of $Bi_{0.75}Er_{0.23}Pr_{0.02}O_{1.5+x}$ ceramics sintered at 600°C from fine fraction < 2 μm of MA nano-powder.

In the development of durable functional materials, the MA of solid-state processes makes it possible to detect and study degradation processes due to fast feedback. When developing technology, negative aspects can be eliminated by using the most appropriate methods and conditions that consider the threshold nature of mechanochemical phenomena. For example, a simple operation of annealing free volume in cermet nano-powders at T ~ 400°C before hot pression drastically reduces the rate of phase degradation [27]. As a result, nano-cermet with *RD* > 0.95 prepared from fine powder fraction successfully passed the phase durability test at 500°C for 500 hours, which is shown in Figures 21 and 22. MCM turned out to be quite suitable for the synthesis of metal matrix composites and alloys, but the average particle size is ~10–30 μm. In this case, the synthesis of nano-cermets from fine fractions for four minutes of MA is already significant for the formation of a free volume in fluorite δ-Bi_2O_3. Preparation of nanocomposite powders with a minimum free volume in ceramic grains by grinding in a liquid medium in bead mills seems to be more promising. In this case, it is possible to avoid the occurrence of negative mechanochemical phenomena and immediately obtain a paste for deposition to the substrate.

4.2.7.10. Smart Oxygen Membrane (A+B+C+D+G)

The creation of an operating membrane obviously requires the chemical and physical compatibility of the contacting materials. However, this is not enough to develop a viable technology. To obtain a gas-tight selective layer from a fine fraction of cermet nano-powder, the required pressure is P = 0.5 – 1 GPa at T = 350 – 400°C, which is quite difficult to achieve for a membrane with a diameter of 20 mm, which is shown in Figure 30.

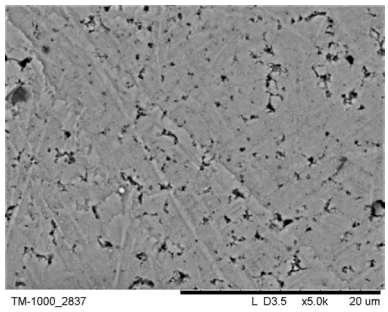

Figure 30: SEM image of nano-cermet 60F/40Ag after HP at 1 GPa and 350°C.

A smart membrane means its variability at different stages of the roadmap, ensuring the transition from the original powders to the operating membrane with technologically feasible parameters. The main role is played by a two-level metal-matrix nanocomposite with a core-shell structure instead of silver in conventional cermet. For instance, nanocomposite $Ag_{0.7}Cu_{0.3}$@($CuMn_2$@$CuMn_2O_4$)($La_{0.7}Y_{0.3}Co_{0.5}Fe_{0.3}Mn_{0.2}O_3$) performs several functions. Ceramic fillers make it possible to obtain powders of heterogeneously doped alloys with a smaller particle size during grinding, as shown in **Figure 31**.

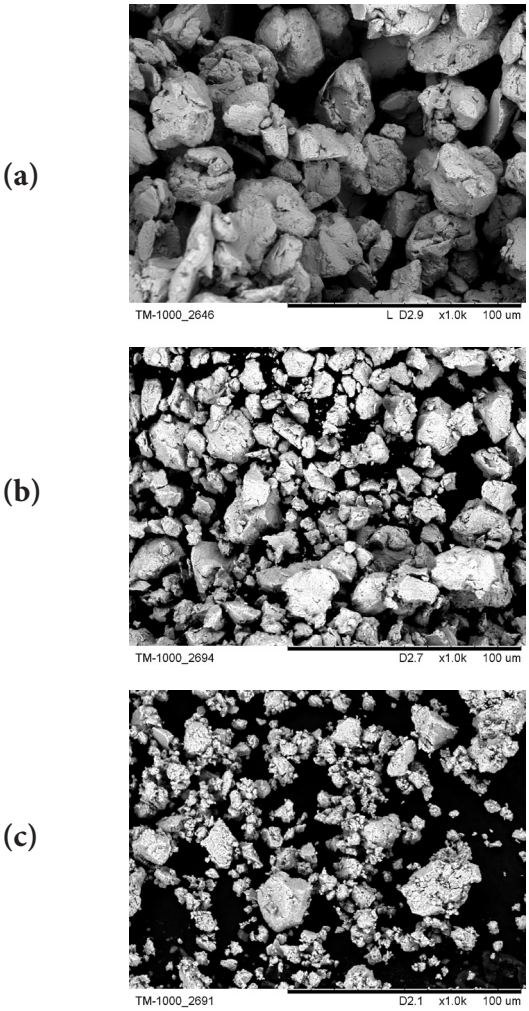

Figure 31: SEM image of powders after mechanical alloying: **(a)** $Ag_{0.7}Cu_{0.3}$, **(b)** $Ag_{0.7}Cu_{0.3}$@ $La_{0.7}Y_{0.3}Co_{0.5}Fe_{0.3}Mn_{0.2}O_3$, **(c)** $Ag_{0.7}Cu_{0.3}$@ $CuMn_2O_4$.

The alloy $Ag_{0.7}Cu_{0.3}$ simultaneously reduces the silver content of the cermet and the cost of the membranes. The increased ductility of the alloy due to the lowered T_m = 820°C (in Ag T_m = 962 °C) reduces the hot consolidation pressure, despite the lowered Ag content in the composite and heterogeneous doping with ceramics. The high wettability of ceramic nano-sized fillers, including spinel and perovskite, provides a rigid framework in the metal matrix that inhibits silver recrystallization and segregation. $CuMn_2$ alloy is oxidized at T ~ 600°C. The formation of spinel $CuMn_2O_4$ with high wettability to silver also leads to dilatation of the metal matrix. The content of the alloy determines the allowable porosity of the cermet after hot consolidation. According to rough estimates, at 10 wt% $CuMn_2$ alloy content, the cermet porosity after oxidation will decrease and the relative density will increase by ~ 0.05, which allows halving the pressing of hot consolidation to 250 MPa at T = 400°C. $CuMn_2O_4$ spinel is capable of absorbing CuO in a significant amount, which occurs during the oxidation of copper in a silver alloy $Ag_{0.7}Cu_{0.3}$. Moreover, the conductive properties of $Cu_{1.33}Mn_{1.67}O_4$ spinel even increase **[49,50]**.

An important position of a smart membrane is the mode of operation. With the stability of fluorite reaching 1,000 hours at 600°C **[43]**, the required durability of membranes in DMG of 8,000 hours at T_o ~ 550°C can be achieved by periodic fast regeneration—7 times at 640°C **[28]**.

4.2.7.11. Optimal Operation Temperature T_o (A+B+C+D+F)

The optimal operating temperature of the OSM is the most important parameter of the ITM technology. A diagram of multidirectional factors that determine the choice of a narrower range of T_o is shown in **Figure 32**. The membrane regeneration temperature is substantiated by the maximum thermal effect at 640°C, caused by the disordering of oxygen vacancies **[51]**. Membrane durability testing is a difficult task with slow feedback, so the accuracy of predictions T_o is very important.

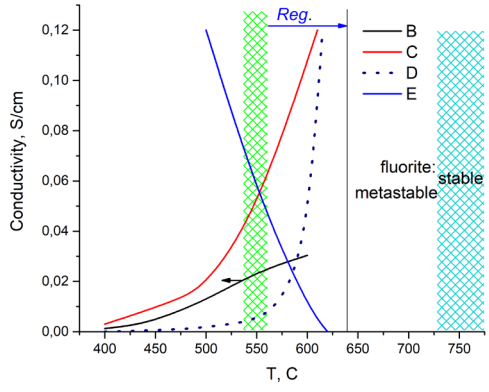

Figure 32: General diagram for determination optimal T_o for cermet. B- conductivity; C- rate recrystallization of fluorite, a. u.; D- probability of nucleation of stable phases, a. u.; E- rate of oxygen vacancy ordering, a. u.; blue area – fluorite stability field; green area – likely range of optimal T_o for IT membrane.

It can be assumed that the strongest factor, the probability of nucleation of stable phases, is the most unpredictable. However, the technology of synthesis is of decisive importance, especially the homogeneity of the doping. This conclusion is based on a significant difference in the phase stability of hafnium-doped fluorite obtained in **[28,43]**, shown in **Figure 26**.

4.2.7.12. Assessing the Viability of ITM Technology Based on Cermet for DMG

The price of the first membrane is determined by the cost of materials and fabrication: $C_{mem} = C_{mat} + C_{fab}$. When implementing DMG with the collection of used membranes and recycling of materials, the cost will tend to $C_{\infty} = C_{rec} + C_{fab}$. At the same time, the cost of recycling membranes with the extraction of expensive elements for re-production is expected to be $C_{rec} << C_{mat}$. Due to the absence of losses of rare elements in the streamlined industrial production of membranes, their low content in the earth's crust will not become a deterrent to the development of DMG.

The calculations will be made with the following parameters: 1) m-TPP from two reactors with thermal power of 13 MW (electric power of ~3.9 MW), consuming 1 kg of fuel per second at 50% carbon content in the fuel. The oxygen demand is 1.33 kg/s, of which 0.84 kg/s falls on the membranes, and the rest is from the air, as shown in **Figure 2**. The flow of oxygen from the membranes is assumed to be 3 ml/min.cm^2 (2.38.10-4 kg/s.m^2), which is a real value, taking into account the small thickness of the membranes and the use of the best Pt(Pd) catalysts for the exchange reactions. Such a flow is provided by perovskite membranes at T_o ~ 750°C **[11]**, at which acceptable durability can be expected. The membrane surface will be 3530 m^2. The cost of reagents is estimated according to the architecture of the membrane shown in **Figure 28** and **Table 2**.

Table 2: Approximate cost of basic reagents per 1 m^2 of membrane on a substrate with a selective layer thickness of 10 μm.

Reagent	Content in earth's crust, ppm	Reserves, 10^3 T	Content for 1 m^2, g	Cost, USD/g	Cost
Ag	0.1	400	17	1	17
Pd	0.01	-	0.05	84	4
Pt	0.2	76	0.05	37	2
Bi_2O_3	0.1	130	50	0.1	5
Co_3O_4	20	56000	50	0.2	10
Dy_2O_3	4		7	0.2	1.4
Er_2O_3	3		7	0.4	1.4
Total					~40

The cost of expensive reagents is ~40 USD/m^2. The cost of membrane fabrication is still difficult to estimate. However, the choice of continuous technology for the membrane fabrication on a 10 cm wide steel mesh substrate guarantees a low price in mass production. One continuous line at a speed of 5 mm/s will provide production of 15,000 m^2/year. The assembly of flat membranes into large modules is incomparably simpler than tubular ones **[11]**. For estimates of C_{fab}, one can take a deliberately overestimated 10-fold cost of C_{mat}, considering that the cost of the first membrane C_{mem} is ~ 400 USD/m^2. When reaching the stationary level of the DMG market (~7% electric power), the cost of membranes will be almost completely determined by the cost of fabrication, $C_{\infty} = C_{rec} + C_{fab} \sim C_{fab}$. It is very important to note that the cost of membranes will not depend on fluctuations in market prices for reagents due to the circulation of rare elements within the DMG technology. For comparison, the cost of 1 m^2 of hydrogen membrane NR211 DuPont NAFION without supported noble metal catalysts is 2500 USD/m^2, and for the viability of perovskite technology, the cost of membranes should be below 1500 USD/m^2 **[11]**. For the first m-TPP, the price of membranes is estimated at ~1,000,000 USD with a deliberately overestimated cost of fabrication.

Full implementation of DMG is achieved with the launch of 10,000 m-TPPs. For this, 600 T of Ag, 1.77 T of Pd, 1.77 T of Pt, 1765 T of Bi_2O_3, and 1765 T of CoO will be consumed. The most significant share falls on Bi_2O_3 - 1.36% of world reserves. For other elements, DMG would require a tiny fraction of the world's reserves to realize its full market potential.

4.2.7.13. Summary of Cermet Membranes

Most of the significant problems with the development of membranes are solved today. Positive changes can be seen when compared with earlier works **[52]**. The use of MA in research has made it possible to reveal slow and hidden processes and understand the degradation. This is the most important thing in the development of durable membranes for energy applications. More research is needed to find a suitable technique for nano-milling of nano-cermets in a liquid medium to avoid a formation of free volume in ceramics, preparation and deposition of supported Pd, Pt-catalyst, further optimization of Ag-filler compositions to reduce interdiffusion, and degradation rates of fluorite. In addition, the investigation of rapid thermal treatment (laser heating and electron irradiation) of raw membranes for the continuous fabrication of membrane sheets is only the start. The technical problems of sealing cermet membranes and assembly of membrane modules have not yet been solved, but there is experience gained in the development of other devices (SOFCs). Membrane assembly is practically the last technological operation before durability testing with subsequent applications. We have participated in mainstream research of oxygen membranes for Catalytic Membrane Reactors (CMR) and SOFC **[32,53–59]**. Such devices are still proposed in numerous energy reviews aimed at decarbonization **[60–63]**. Despite the progress made in creating tubular CMR with a multilayer architecture based on MIEC perovskites, we stopped research in this direction due to the impossible scaling of the technology related to complicated assembling. All the numerous energy review papers on the combustion of fuel in an oxygen atmosphere with carbon dioxide sequestration gloss over insurmountable problems such as scaling or degradation and the scarcity of

resources (noble metals, REE, etc). In our case, it is especially important to note that due to the potentially low cost of continuous fabrication of thin flat membranes, there is a significant possibility to increase the durability of membranes by lowering T_o below 550°C. In this case, the decrease in the specific productivity of membrane modules is easily compensated by an increase in their surface.

5. Conclusions

Global challenges such as environmental pollution, social inequality, lack of energy, and other resources have conjugated and balanced scientific and technical depoliticized solutions. The UN-HABITAT program can make a significant contribution to sustainable development. The synergistic combination of eco-settlements and DMG based on IT OSM cermet technology fully meet modern challenges. A successfully implemented pilot project of a semi-autonomous eco-estate with a two-fold reduction in capital and maintenance costs in a harsh climate shows the prospects for the mass dissemination of eco-villages. The development of autonomous eco-settlements based on DMG provides an opportunity for reasonable de-urbanization, which reduces the fragility of the modern complex structure of the economy and society, along with the preservation of the environment and the efficient use of all types of resources, including sun and wind energy. Membrane-based technology for pulverized solid fuel combustion in an oxygen-enriched atmosphere can ensure the rational use of practically unlimited natural carbon resources (coal, shales, etc.). Understanding physical and chemical processes, especially membrane degradation, allows for formulating solutions for the development and implementation of IT OSM technology. Optimization of the composition of metastable fluorite by minor dopants and replacing silver in δ-Bi_2O_3/Ag cermet with a metal-matrix composite makes it possible to realize the ideas of a smart membrane with reduced cost, increased durability, and technical feasibility. The complex problem of recrystallization and segregation of Ag in cermet, leading to the total degradation of membranes, is solved by heterogeneous doping of silver with Cu, Mn-spinel, which has excellent wettability due to the high electronic conductivity of ceramics and topotaxy. The natural resources of rare elements are sufficient for the full implementation of DMG. Moreover, some rare volatile elements can be collected in significant quantities.

Data Availability

The data supporting the findings of this study are available within the article and in reference numbers **[28,33,41]**.

Conflicts of Interest

The author declares that there is no conflicts of interest.

Funding

This work was supported by the Russian Foundation for Basic Research, Grant 20-03-00349, and within the framework of the state assignment of the Institute of Solid State Chemistry and Mechanochemistry, Siberian Branch of Russian Academy of Sciences (Project 0301-2019-0002).

References

[1] Ecovillages Archive. Global Ecovillage Network n.d. https://ecovillage.org/projects/.

[2] A Better Urban Future | UN-Habitat n.d. https://unhabitat.org/ (accessed February 4, 2022).

[3] Новости РИА. [About 200 ecovillages have emerged in the Russian Federation over the past 20 years]. РИА Новости 20121030T1407. https://ria.ru/20121030/907922866.html (accessed February 9, 2022).

[4] Zyryanov VV, Sysoev VF, Boldyrev VV, Korosteleva TV. USSR inventor's certificate No. 1375 328. Byull Izobret 1988:39.

[5] Zyryanov V. Processing of oxide ceramic powders for nanomaterials using high-energy planetary mills. InterCeram 2003;52:22–7.

[6] Zyryanov VV, Zyryanov DV. [Fly Ash as —Technogenic Raw Material]. Moscow: OOO IPTs-Maska; 2009.

[7] Zyryanov VV. Mechanoemission and Related Phenomena – Electron-Hole Ferromagnetism in Nonmagnetic Dielectrics and Gas-Dusty Plasma. Possible Applications. Chemistry for Sustainable Development 2019;27:217–28. https://doi.org/10.15372/CSD2019130.

[8] Zyryanov VV, Zyryanov DV. Complex Processing of Pulverized Fly Ash by Dry Separation Methods. Journal of Environmental Protection 2010;1:293–301. https://doi.org/10.4236/jep.2010.13035.

[9] Zyryanov VV, Zyryanov DV, Sadykov VA. Fabrication of coatings by the charged aerosol deposition method. Nanotechnol Russia 2008;3:311. https://doi.org/10.1134/S1995078008050066.

[10] Zyryanov VV. Composition for stabilizing clay ground and method for creating ground roads with its use. RU2592588C1, 2015.

[11] Den Exter MJ, Haije WG, Vente JF. Viability of ITM technology for oxygen production and oxidation processes: Material, system, and process aspects. Inorg. Membranes for Ener. and Environ. Applic., Springer New York; 2009, p. 27–51. https://doi.org/10.1007/978-0-387-34526-0_2.

[12] Kotlyakov VM. Global causes and effects of the climate change and glaciations on the Earth (A review). IOP Conf Ser: Earth Environ Sci 2010;13:012001. https://doi.org/10.1088/1755-1315/13/1/012001.

[13] Smith SJ, van Aardenne J, Klimont Z, Andres RJ, Volke A, Delgado Arias S. Anthropogenic sulfur dioxide emissions: 1850–2005. Atmospheric Chemistry and Physics 2011;11:1101–16. https://doi.org/10.5194/acp-11-1101-2011.

[14] Fleming LN, Abinteh HN, Inyang HI. Leachant pH effects on the leachability of metals from fly ash. Journal of Soil Contamination 1996;5:53–9. https://doi.org/10.1080/15320389609383512.

[15] Walter KM, Zimov SA, Chanton JP, Verbyla D, Chapin FS. Methane bubbling from Siberian thaw lakes as a positive feedback to climate warming. Nature 2006;443:71–5. https://doi.org/10.1038/nature05040.

[16] Equitable future cities hold answers to pollution, climate and nature breakdown | UN-Habitat n.d. https://unhabitat.org/

equitable-future-cities-hold-answers-to-pollution-climate-and-nature-breakdown (accessed February 4, 2022).

[17] The Potential for Carbon Sequestration in the United States:https://www.cbo.gov/sites/default/files/110th-congress-2007-2008/reports/09-12-carbonsequestration.pdf.

[18] [Coal - Futures contract - Prices | 2008-2022 Data | 2023-2024 forecast] n.d. https://ru.tradingeconomics.com/commodity/coal (accessed February 9, 2022).

[19] Jones N. How dangerous is Africa's explosive Lake Kivu? https://www.nature.com/immersive/d41586-021-02523-5/index.html (accessed February 9, 2022).

[20] Ten Elshof JE, Nguyen NQ, Den Otter MW, Bouwmeester HJM. Oxygen permeation properties of dense Bi1.5Er0.5O3-Ag cermet membranes. J Electrochem Soc 1997;144:4361–6. https://doi.org/10.1149/1.1838194.

[21] Chen CS, Kruidhof H, Bouwmeester HJM, Verweij H, Burggraaf AJ. Thickness dependence of oxygen permeation through erbiastabilized bismuth oxide-silver composites. Solid State Ionics 1997;99:215–9. https://doi.org/10.1016/s0167-2738(97)00271-3.

[22] Chen CS, Burggraaf AJ. Stabilized bismuth oxide–noble metal mixed conducting composites as high temperature oxygen separation membranes. Journal of Applied Electrochemistry 1999;29:355–60. https://doi.org/10.1023/A:1003448704121.

[23] Fedorov SV, Lysenkov AS, Kulbakin IV. Reactionary-solidified oxygen permeable membrane material based on cermet Bi1.6Er0.4O3 – 26 wt % Ag – 4 wt % In. IOP Conf Ser: Mater Sci Eng 2020;848:012019. https://doi.org/10.1088/1757-899X/848/1/012019.

[24] Zyryanov VV, Matvienko AA. Effect of surface modification with Au, Pd, and Pt on the morphology of δ-Bi_2O_3/Ag-based nanocermets. Inorg Mater 2015;51:362–8. https://doi.org/10.1134/S002016851503019X.

[25] Zyryanov VV, Petrov SA, Ulihin AS. Mechanically activated synthesis, characterization and conducting properties of complex perovskites for Ag-based metal-matrix nanocomposites. Ceram Int 2021;47:29499–503. https://doi.org/10.1016/j.ceramint.2021.07.118.

[26] Zyryanov VV, Ulihin AS, Bulina NV, Matvienko AA, Maslennikov DV, Popov MP. Combination of potential nanomaterials for intermediate temperature oxygen membranes on the base of δ-Bi_2O_3/Ag. Mater Today Proc 2019;12:30–4. https://doi.org/10.1016/j.matpr.2019.03.013.

[27] Zyryanov VV. New nanomaterials and nanoarchitecture of oxygen membranes for clean energy. Mater Today Proc 2019;25:416–9. https://doi.org/10.1016/j.matpr.2019.12.138.

[28] Zyryanov VV, Ulihin AS. Understanding δ-Bi_2O_3 fluorite degradation mechanism and related solutions for promising applications in distributed multigeneration. Ceram Int 2022;48:16877–84. https://doi.org/10.1016/j.ceramint.2022.02.242.

[29] Jiang N, Buchanan RM, Henn FEG, Marshall AF, Stevenson DA, Wachsman ED. Aging phenomenon of stabilized bismuth oxides. Mater Res Bull 1994;29:247–54. https://doi.org/10.1016/0025-5408(94)90020-5.

[30] Boyapati S, Wachsman ED, Chakoumakos BC. Neutron diffraction study of occupancy and positional order of oxygen ions in phase stabilized cubic bismuth oxides. Solid State Ionics 2001;138:293–304. https://doi.org/10.1016/S0167-2738(00)00792-X.

[31] Wachsman ED. Effect of oxygen sublattice order on conductivity in highly defective fluorite oxides. J Eur Ceram Soc 2004;24:1281–5. https://doi.org/10.1016/S0955-2219(03)00509-0.

[32] Zyryanov VV, Uvarov NF, Sadykov VA, Ulihin AS, Kostrovskii VG, Ivanov VP, *et al.* Mechanochemical synthesis and conducting properties of nanostructured rhombohedral scandia stabilized zirconia ceramics. J Alloys Compd 2009;483:535–9. https://doi.org/10.1016/j.jallcom.2008.07.229.

[33] Zyryanov VV, Petrov SA. Transformation of fluorite δ-Bi_2O_3 into a new tetragonal phase. J Serb Chem Soc (In press).

[34] Zyryanov VV. Smart oxygen membranen p. MATEC Web Conf 2021;340. https://doi.org/10.1051/matecconf/202134001039.

[35] Sadykov V, Mezentseva N, Arapova M, Krieger T, Gerasimov E, Alikina G, *et al.* Fast oxygen transport in bismuth oxide containing nanocomposites. Solid State Ionics 2013;251:34–9. https://doi.org/10.1016/j.ssi.2013.03.016.

[36] Steacie EWR, Johnson FMG, Eve AS. The solubility and rate of solution of oxygen in silver. Proceedings of the Royal Society of London Series A, Containing Papers of a Mathematical and Physical Character 1926;112:542–58. https://doi.org/10.1098/rspa.1926.0128.

[37] Kim JS, Kuk E, Yu KN, Kim J-H, Park SJ, Lee HJ, *et al.* Antimicrobial effects of silver nanoparticles. Nanomedicine: Nanotechnology, Biology and Medicine 2007;3:95–101. https://doi.org/10.1016/j.nano.2006.12.001.

[38] Fellah MF, van Santen RA, Onal I. Epoxidation of Ethylene by Silver Oxide (Ag2O) Cluster: A Density Functional Theory Study. Catal Lett 2011;141:762–71. https://doi.org/10.1007/s10562-011-0614-2.

[39] Zyryanov VV. Ultrafast mechanochemical synthesis of mixed oxides. Inorg Mater 2005;41:378–92. https://doi.org/10.1007/s10789-005-0140-y.

[40] Zyryanov VV. Mechanochemical synthesis of complex oxides. Russ Chem Rev 2008;77:105–35. https://doi.org/10.1070/RC2008v077n02ABEH003709.

[41] Zyryanov VV. Mechanically assisted chemical interaction of doped bismuth oxide with silver. Solid State Ionics 2022;383:115987. https://doi.org/10.1016/j.ssi.2022.115987.

[42] Yukhin YM, Mikhailov YI. Chemistry of bismuth compounds and materials. Novosibirsk, SO RAN: 2001.

[43] Yun B-H, Lee C-W, Jeong I, Lee KT. Dramatic Enhancement of Long-Term Stability of Erbia-Stabilized Bismuth Oxides via Quadrivalent Hf Doping. Chem Mater 2017;29:10289–93. https://doi.org/10.1021/acs.chemmater.7b03894.

[44] Kouamé BSR, Baranton S, Brault P, Canaff C, Chamorro-Coral W, Caillard A, *et al.* Insights on the unique electro-catalytic behavior of PtBi/C materials. Electrochimica Acta 2020;329:135161. https://doi.org/10.1016/j.electacta.2019.135161.

[45] Nan B, Fu Q, Yu J, Shu M, Zhou L-L, Li J, *et al.* Unique structure of active platinum-bismuth site for oxidation of carbon monoxide. Nat Commun 2021;12:3342. https://doi.org/10.1038/s41467-021-23696-7.

[46] Kargin YuF, Egorysheva AV, Volkov VV, Burkov VI, Shandarov SM, Mandel AE, *et al.* Growth and characterization of doped Bi12TiO20 single crystals. Journal of Crystal

Growth 2005;275:e779–84. https://doi.org/10.1016/j.jcrysgro.2004.11.093.

[47] Harwig HA, Gerards AG. Electrical properties of the α, β, γ, and δ phases of bismuth sesquioxide. Journal of Solid State Chemistry 1978;26:265–74. https://doi.org/10.1016/0022-4596(78)90161-5.

[48] Zyryanov VV. Mechanism of mechanochemical synthesis of complex oxides and the peculiarities of their nano-structurization determining sintering. Sci Sinter 2005;37:77–92. https://doi.org/10.2298/SOS0502077Z.

[49] Petric A, Ling H. Electrical conductivity and thermal expansion of spinels at elevated temperatures. J Am Ceram Soc 2007;90:1515–20. https://doi.org/10.1111/j.1551-2916.2007.01522.x.

[50] Martin BE, Petric A. Electrical properties of copper–manganese spinel solutions and their cation valence and cation distribution. Journal of Physics and Chemistry of Solids 2007;68:2262–70. https://doi.org/10.1016/j.jpcs.2007.06.019.

[51] Tran TB, Navrotsky A. Energetics of disordered and ordered rare earth oxide-stabilized bismuth oxide ionic conductors. Phys Chem Chem Phys 2014;16:2331–7. https://doi.org/10.1039/c3cp54553a.

[52] Zyryanov VV. Possibilities of creating a pure coal-fired power industry based on nanomaterials. Therm Eng 2015;62:577–85. https://doi.org/10.1134/S0040601515040114.

[53] Zyryanov VV, Uvarov NF, Kostrovskii VG, Sadykov VA, Kuznetsova TG, Rogov VA, *et al*. Design of New Oxide Ceramic Materials and Nanocomposites with Mixed Conductivity by Using Mechanical Activation Route. Mater Res Soc Symp Proc, vol. 755, 2003, p. 271–6.

[54] Zyryanov VV, Uvarov NF, Sadykov VA, Frolova YV, Alikina GM, Lukashevich AI, *et al*. Mechanosynthesis of complex oxides and preparation of mixed conducting nanocomposites for catalytic membrane reactors. Catal Today 2005;104:114–9. https://doi.org/10.1016/j.cattod.2005.03.047.

[55] Zyryanov VV, Sadykov VA, Uvarov NF, Alikina GM, Lukashevich AI, Neophytides S, *et al*. Mechanosynthesis of complex oxides with fluorite and perovskite-related structures and their sintering into nanocomposites with mixed ionic-electronic conductivity. Solid State Ionics 2005;176:2813–8. https://doi.org/10.1016/j.ssi.2005.08.011.

[56] Zyryanov VV, Sadykov VA. Design of multilayered ceramic MIEC membranes. Desalination 2006;199:299–301. https://doi.org/10.1016/j.desal.2006.03.176.

[57] Zyryanov VV, Sadykov VA, Alikina GM. Design of multilayer ceramic MIEC membranes. Sep Sci Technol 2007;42:2849–61. https://doi.org/10.1080/01496390701558300.

[58] Zyryanov VV. Fabrication of multilayer ceramic membranes. Asia-Pac J Chem Eng 2009;4:285–90. https://doi.org/10.1002/apj.244.

[59] Zyryanov VV, Nemudry AP, Sadykov VA. Nanostructured Perovskites for the Fabrication of Thin Ceramic Membranes and Related Phenomena. Membranes for Membr. React.: Prep., Optim. and Selection, John Wiley and Sons; 2011, p. 201–25. https://doi.org/10.1002/9780470977569.ch6.

[60] Habib MA, Badr HM, Ahmed SF, Ben-Mansour R, Mezghani K, Imashuku S, *et al*. A review of recent developments in carbon capture utilizing oxy-fuel combustion in conventional and ion transport membrane systems. International Journal of Energy Research 2011;35:741–64. https://doi.org/10.1002/er.1798.

[61] Habib MA, Nemitallah M, Ben-Mansour R. Recent Development in Oxy-Combustion Technology and Its Applications to Gas Turbine Combustors and ITM Reactors. Energy Fuels 2013;27:2–19. https://doi.org/10.1021/ef301266j.

[62] Habib MA, Nemitallah MA. Design of an ion transport membrane reactor for application in fire tube boilers. Energy 2015;81:787–801. https://doi.org/10.1016/j.energy.2015.01.029.

[63] Yadav S, Mondal SS. A review on the progress and prospects of oxy-fuel carbon capture and sequestration (CCS) technology. Fuel 2022;308:122057. https://doi.org/10.1016/j.fuel.2021.122057.

How to Cite

Zyryanov VV. Intermediate Temperature Oxygen Selective Membrane Technology Based on δ-Bi_2O_3/Ag Cermet for Distributed Multigeneration in Eco-Settlements with Sustainable Development. Membrane Sci Int 2022;1(2):24–43.